Supplementary material for "Rethinking Ytterbium(III)-based Single-Molecule Magnets – Why Trigonal Planar Doesn't Work!"

Vinicius Fagundes, [a] Egidio Dias Viegas,[a] and Marcus J. Giansiracusa*[a]

Contents:

1. Literature SMM data

Table S1. Collection of Er zero-field SMMs in literature.

Er(III) SMMs	U_{eff} **(K)**	**Magnetic Field (Oe)**	**Ref**
$[Er(dbpc)_3]$	55.7	0	32
$[Er(btmsm)_3]$	114.5	0	32
$[Er\{N(SiMe_3)_2\}_3]$	122	0	33
$[Li(THF)_4][Er\{N(SiMe_3)_2)_3Cl]$	63.3	0	34
$[K(18\text{-crown-}6)][Er(COT)_2]$	216	0	35
$[K_2(THF)_4][Er_2(COT'')_3]$	306	0	36
$[Er_2(COT'')_3]$	323	0	36
$K_2(THF)_4[Er_2(COT)_4]$	286	0	36
$(C_5H_5BMe)Er(COT)$	421	0	37
$(C_5H_5BH)Er(COT)$	371	0	37
$[Er(COT)(C_5H_5BNEt_2)]$	250	0	37
Er(COT)I(DMPE)	108	0	38
(Cp*)Er(COT)	323; 197 (slow/fast)	0	39
Er(COT)(Dsp)	358	0	40
$[Li(DME])_3][Er(COT'')_2]$	187	0	41
$[K(18\text{-crown-}6)][Er(COT)_2]$	286	0	42

$dbpc^-$ = tris(2,6-di-tert-butyl-p-cresolate); btmsm = tris(bis(trimethylsilyl)methyl) radical; COT = cyclooctatetraenide; DMPE = 1,2-Bis(dimethylphosphino)ethane; Dsp = 3,4- dimethyl-2,5-bis(trimethylsilyl)phospholyl, COT" = 1,4-bis(trimethylsilyl)cyclooctatetraenyl and Cp = pentamethylcyclopenta-dienyl.

Table S2. Continuation of literature Yb(III)-based SMMs

Compound	U_{eff}/k_B (K)	H_{dc} (Oe)	Ref
$[Yb(2,2'\text{-bipyridine-}1,1'\text{-dioxide})_4]$ - M-CN bridged	9.4-20.6	800-1500	1
$[Yb(OPAd_2Bz)_2(H_2O)_4Cl]Cl_2\cdot 2THF$	18.77	1000	2
$Yb_4(Hquinha)_8(C_2H_5OH)_2(H_2O)_6](ClO_4)_4\cdot 4C_2H_5OH\cdot H_2O$	9.2-12.5	1000	3
$[Yb(QR1)(tta)_2]\cdot CH_3OH$	16.1	1000	4
$[\{Yb(apdo)\text{-}(H_2O)_4\}\{Co(CN)_6\}]\cdot 2H_2O$	15.8	700	5
$[Yb(H_3Bmshp)(DMF)_2Cl_2]\cdot DMF\cdot 1.5H_2O$	14.5	1500	6
$[Yb(\mu_3\text{-}OH)(na)(pyzc)]_n$	14.4	3000	7
$[YbL_3]\cdot CH_3OH$	11.7	1000	8
$[YbL]_2(OTf)_2](OTf)$	11.7	1000	9
$\beta\text{-}Yb(2\text{-}qpH)(SO_4)(H_2O)_2$	11.5	2000	10
$[Yb_2(hfac)_6(H_2SQ)]\cdot 0.5CH_2Cl_2$	10	800	11
$[Yb(2,2'\text{-bpdo})_2(H_2O)][Cu_2(CN)_5]\cdot 5H_2O$	9.2	1000	12
$[Yb(Ph_3PO)_4(NO_3)_2](NO_3)$	9.2	2500	13
$[YbZn_2(SS/RR\text{-}L)_2(H_2O)_4](ClO_4)_3\cdot 5H_2O$	8.94	1000	14
$[YbFc_3(THF)_2Li_2]^-$	8.6	2000	15
$(Et_3NH)[Yb(3\text{-}NO_2\text{-salen})]$	7.5	1500	16
$[Yb_2(2\text{-}FBz)_6(phen)_2]$	7.2	2000	17
$[Yb(H_3L)_2]Cl_3\cdot 5CH_3OH.2H_2O$	7	400	18
$[Yb(tta)_3L]\cdot 2CH_2Cl_2$	6	1000	19
$[Yb(H_2O)_3(18\text{-crown-}6)](ClO_4)_3$	5.9	500	20
$[Yb(QR1)_2][NO_3]\cdot (CH_3OH)(H_2O)_{0.5}$	5.37	1000	4
$[YbTp_2NO_3]$	No fitting	2000	21
$[N(C_2H_5)_4]_3[Yb(dipic)_3].nH_2O$	No fitting	1000	22
$\{[Yb(hfac)_3((S)\text{-}L^1)]_3\}_n$	Raman fit	1000	23
$\{[Yb(hfac)_3((S,S,S)\text{-}L^2)]_3\}_n$	Raman fit	1000	23
$\{[Yb(hfac)_3((S)\text{-}L^3)]_3\}_n$	Raman fit	1000	23
$\{[Yb(hfac)_3((S,S,S)\text{-}L^4)]_3\}_n$	Raman fit	1000	23
$[Yb\{N(SiMe_3)_2\}_3]$	Raman + QTM	1700	24
$[Yb\{N(SiMe_2H)_2\}_3\cdot(thf)_2]$	Raman + QTM	1700	24
$[Yb\{N(SiMePh_2)_2\}_2][Al\{OC(CF_3)_3\}_4]$	Raman + Direct	1600	25
$\{Yb(4\text{-pyridone})_4[Fe(phen)_2(CN)_2]_2\}(CF_3SO_3)_3\cdot solv$	Raman + Direct	800	26
$[YbCl_3tpa]$	Raman + Direct	2000	27
$[Yb(NO_3)_3tpa]$	Raman + Direct	2000	27
$[Yb_4(bpzch)_2(fod)_{10}]$	Raman	1500	28
$[YbCo(CN)_6(bpyO_2)_2(H_2O)_3]\cdot 4H_2O$	Raman	1250	29
$[Yb(Br_4Hcat)_3tpa]$	Raman	1000	30
$[Yb(TPPO)_3(NCS)_3]/[Yb(TPPO)_3(NCSe)_3]$	No Peaks	up to 4000	31

2. Idealised Structure calculation for Yb(III) and Er(III)

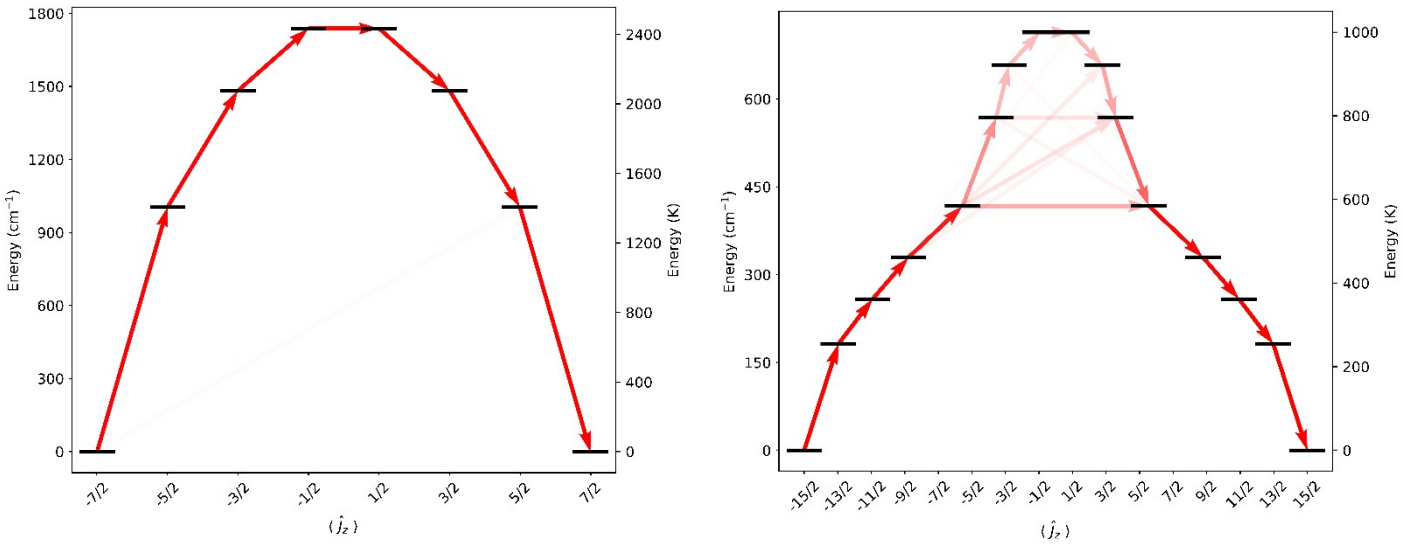

Figure S1. An energy barrier plot illustrating the relaxation process for YbF_3 (left) and ErF_3 (right).

Table S3. The expectation values for the probable transitions of wavefunction mixing for YbF_3.

States	WF1	WF2	WF3	WF4
WF2	1.000			
WF3	0.000	1.320		
WF4	0.000	0.000	1.470	
WF-4	0.000	0.000	0.000	1.500
WF-3	0.042	0.000	0.000	0.000
WF-2	0.074	0.068	0.000	0.000
WF-1	0.071	0.074	0.042	0.000

Table S4. Crystal field properties resulted from CASSCF-SO calculations for an idealised ErF_3 molecule in D_{3h} point group symmetry.

Crystal field		***g*-tensor values**			**Angle**	**Wavefunction decomposition**
Energy (cm^{-1})	**Energy (K)**	g_x	g_y	g_z	(°)	
0	0	2.39×10^{-8}	2.75×10^{-8}	17.91	--	100%$\lvert \pm 15/2\rangle$
181	261	2.35×10^{-1}	2.35×10^{-1}	15.47	0	99.8%$\lvert \pm 13/2\rangle$; 0.2% $\lvert \pm 1/2\rangle$
259	372	2.04×10^{-1}	2.04×10^{-1}	13.03	0	99.4%$\lvert \pm 11/2\rangle$; 0.6% $\lvert \mp 1/2\rangle$
329	474	7.78×10^{-6}	1.74×10^{-5}	10.46	0	98.2%$\lvert \pm 9/2\rangle$; 1.8% $\lvert \mp 3/2\rangle$
417	600	5.83	5.83	6.58	0	88%$\lvert \pm 7/2\rangle$; 12% $\lvert \mp 5/2\rangle$
568	818	5.82	5.82	4.18	0	88%$\lvert \pm 5/2\rangle$; 12% $\lvert \mp 7/2\rangle$
657	946	6.35×10^{-5}	9.29×10^{-5}	3.28	0	98.1%$\lvert \pm 3/2\rangle$; 1.8% $\lvert \mp 9/2\rangle$
714	1027	9.52	9.52	1.12	0	99.2%$\lvert \pm 1/2\rangle$; 0.6% $\lvert \mp 11/2\rangle$; 0.2%$\lvert \pm 13/2\rangle$

Table S5. The expectation values for the probable transitions of wavefunction mixing for ErF_3.

States	WF1	WF2	WF3	WF4	WF5	WF6	WF7	WF8
WF2	1.55							
WF3	0.00	2.11						
WF4	0.00	0.00	2.49					
WF5	0.00	0.00	0.00	2.71				
WF6	0.05	0.00	0.00	0.00	2.23			
WF7	0.04	0.10	0.00	0.00	0.00	3.00		
WF8	0.01	0.10	0.15	0.00	0.00	0.00	3.15	
WF-8	0.00	0.02	0.18	0.24	0.00	0.00	0.00	3.17
WF-7	0.00	0.00	0.10	0.32	0.72	0.00	0.00	0.01
WF-6	0.00	0.00	0.00	0.56	0.78	1.94	0.00	0.02
WF-5	0.02	0.00	0.00	0.00	1.94	0.78	0.72	0.00
WF-4	0.01	0.05	0.00	0.0	0.01	0.56	0.32	0.24
WF-3	0.02	0.09	0.07	0.00	0.00	0.00	0.10	0.18
WF-2	0.00	0.08	0.09	0.05	0.00	0.00	0.00	0.02
WF-1	0.00	0.00	0.02	0.01	0.02	0.00	0.00	0.00

Table S6. Crystal field properties resulted from CASSCF-SO calculations for an idealised YbF_4 molecule in D_{4h} point group symmetry.

Crystal field		***g*-tensor values**			**Angle**	**Wavefunction decomposition**
Energy (cm^{-1})	**Energy (K)**	**g_x**	**g_y**	**g_z**	(°)	
0	0	2.91×10^{-2}	2.91×10^{-2}	7.89	--	99.3%$\vert \pm 7/2\rangle$; 0.7% $\vert \mp 1/2\rangle$
1356	1951	2.05	2.05	4.95	0	92.7%$\vert \pm 5/2\rangle$; 7.3% $\vert \mp 3/2\rangle$
2114	3041	2.07	2.07	2.72	0	92.7%$\vert \pm 3/2\rangle$; 7.3% $\vert \mp 5/2\rangle$
2433	3500	4.52	4.52	1.05	0	99.3%$\vert \pm 1/2\rangle$; 0.7% $\vert \mp 7/2\rangle$

Table S7. Crystal field properties resulted from CASSCF-SO calculations for an idealised ErF_4 molecule in D_{4h} point group symmetry.

Crystal field		***g*-tensor values**			**Angle**	**Wavefunction decomposition**
Energy (cm^{-1})	**Energy (K)**	**g_x**	**g_y**	**g_z**	(°)	
0	0	8.94×10^{-3}	8.94×10^{-3}	17.81	--	99.1%$\vert \pm 15/2\rangle$; 0.9%$\vert \pm 7/2\rangle$
275	395	2.24×10^{-2}	2.24×10^{-2}	15.37	0	99.0%$\vert \pm 13/2\rangle$; 0.9%$\vert \pm 5/2\rangle$; 0.1%$\vert \mp 3/2\rangle$
376	541	0.170	0.170	13.06	0	99.6%$\vert \pm 11/2\rangle$; 0.3%$\vert \pm 3/2\rangle$; 0.1% $\vert \mp 5/2\rangle$
437	629	4.73	4.73	8.71	0	86.4%$\vert \pm 9/2\rangle$; 7.1% $\vert \mp 7/2\rangle$; 6.4%$\vert \pm 1/2\rangle$; 0.1% $\vert \mp 15/2\rangle$
548	789	4.27	4.27	5.50	0	90.3%$\vert \pm 7/2\rangle$; 11.3% $\vert \mp 9/2\rangle$; 7.7% $\vert \mp 1/2\rangle$; 0.8%$\vert \pm 15/2\rangle$;
603	868	8.65	8.65	2.73	0	64.8%$\vert \pm 5/2\rangle$; 34.0% $\vert \mp 3/2\rangle$; 1%$\vert \pm 13/2\rangle$; 0.3% $\vert \mp 11/2\rangle$
1083	1559	8.77	8.77	0.286	0	65.6%$\vert \pm 3/2\rangle$; 34.2% $\vert \mp 5/2\rangle$; 0.1% $\vert \mp 13/2\rangle$
1094	1574	9.08	9.08	0.280	0	85.9%$\vert \pm 1/2\rangle$; 11.8% $\vert \mp 7/2\rangle$; 2.4%$\vert \pm 13/2\rangle$

Table S8. Crystal field properties resulted from CASSCF-SO calculations for an idealised YbF_5 molecule in D_{5h} point group symmetry.

Crystal field		***g*-tensor values**			**Angle**	**Wavefunction**
Energy (cm^{-1})	**Energy (K)**	**g_x**	**g_y**	**g_z**	(°)	**decomposition**
0	0	2.85×10^{-6}	2.85×10^{-6}	7.96	--	$100\%\lvert \pm 7/2\rangle$
1598	2300	2.15×10^{-6}	7.43×10^{-6}	5.59	0	$100\%\lvert \pm 5/2\rangle$
2386	3433	8.04×10^{-7}	1.02×10^{-5}	3.37	0	$100\%\lvert \pm 3/2\rangle$
2815	4051	4.54	4.54	1.10	0	$100\%\lvert \pm 1/2\rangle$

Table S9. Crystal field properties resulted from CASSCF-SO calculations for an idealised ErF_5 molecule in D_{5h} point group symmetry.

Crystal field		***g*-tensor values**			**Angle**	**Wavefunction**
Energy (cm^{-1})	**Energy (K)**	**g_x**	**g_y**	**g_z**	(°)	**decomposition**
0	0	1.26×10^{-9}	1.45×10^{-9}	17.90	--	$100\%\lvert \pm 15/2\rangle$
326	469	1.08×10^{-8}	1.27×10^{-8}	15.47	0	$100\%\lvert \pm 13/2\rangle$
450	648	1.69×10^{-2}	1.69×10^{-2}	13.10	0	$100\%\lvert \pm 11/2\rangle$
558	802	1.69×10^{-2}	1.69×10^{-2}	10.70	0	$100\%\lvert \pm 9/2\rangle$
710	1022	4.21×10^{-5}	4.33×10^{-5}	8.28	0	$100\%\lvert \pm 7/2\rangle$
893	1284	3.60×10^{-5}	4.93×10^{-5}	5.88	0	$100\%\lvert \pm 5/2\rangle$
1058	1523	1.55×10^{-5}	2.88×10^{-5}	3.51	0	$100\%\lvert \pm 3/2\rangle$
1157	1665	9.54	9.54	1.16	0	$100\%\lvert \pm 1/2\rangle$

Table S10. Crystal field properties resulted from CASSCF-SO calculations for an idealised YbF_6 molecule in D_{6h} point group symmetry.

Crystal field		***g*-tensor values**			**Angle**	**Wavefunction**
Energy (cm^{-1})	**Energy (K)**	**g_x**	**g_y**	**g_z**	(°)	**decomposition**
0	0	0.821	0.821	7.73	--	$98.5\%\lvert \pm 7/2\rangle$; $1.5\% \lvert \mp 5/2\rangle$
1992	2866	0.771	0.771	5.36	0	$98.5\%\lvert \pm 5/2\rangle$; $1.5\% \lvert \mp 7/2\rangle$
2918	4198	1.74×10^{-6}	6.27×10^{-6}	3.36	0	$100\%\lvert \pm 3/2\rangle$

3419	4919	4.54	4.54	1.10	0	100%$\vert \pm 1/2\rangle$

Table S11. Crystal field properties resulted from CASSCF-SO calculations for an idealised ErF_6 molecule in D_{6h} point group symmetry.

Crystal field		***g*-tensor values**			**Angle**	**Wavefunction decomposition**
Energy (cm^{-1})	**Energy (K)**	**g_x**	**g_y**	**g_z**	(°)	
0	0	1.42×10^{-7}	9.51×10^{-7}	17.79	--	99.4%$\vert \pm 15/2\rangle$; 0.5%$\vert \pm 3/2\rangle$; 0.1%$\vert \mp 9/2\rangle$
339	487	3.58	3.58	12.83	0	88.5%$\vert \pm 13/2\rangle$; 6.9%$\vert \mp 11/2\rangle$; 4.6%$\vert \pm 1/2\rangle$
470	676	3.22	3.22	9.80	0	86.4%$\vert \pm 11/2\rangle$; 9.3%$\vert \mp 13/2\rangle$; 4.2%$\vert \mp 1/2\rangle$
521	749	2.35×10^{-5}	1.26×10^{-4}	8.31	0	83.7%$\vert \pm 9/2\rangle$; 16.0%$\vert \mp 7/2\rangle$; 0.3%$\vert \mp 15/2\rangle$
573	824	8.56	8.56	3.17	0	64.0%$\vert \pm 7/2\rangle$; 36.0%$\vert \mp 5/2\rangle$
1357	1952	8.51	8.51	0.78	0	64.0%$\vert \pm 5/2\rangle$; 36.0%$\vert \mp 7/2\rangle$
1423	2047	1.67×10^{-5}	1.64×10^{-4}	1.23	0	83.5%$\vert \pm 3/2\rangle$; 16.2%$\vert \mp 9/2\rangle$; 0.3%$\vert \pm 15/2\rangle$
1484	2135	9.16	9.16	0.509	0	91.2%$\vert \pm 1/2\rangle$; 6.7%$\vert \mp 11/2\rangle$; 2.1%$\vert \pm 13/2\rangle$

Figure S2. Energy barrier for an idealised YbF_8 molecule in D_{4d} point group symmetry with a Z-displacement of 0.5 Å and plane angles of 73.8°.

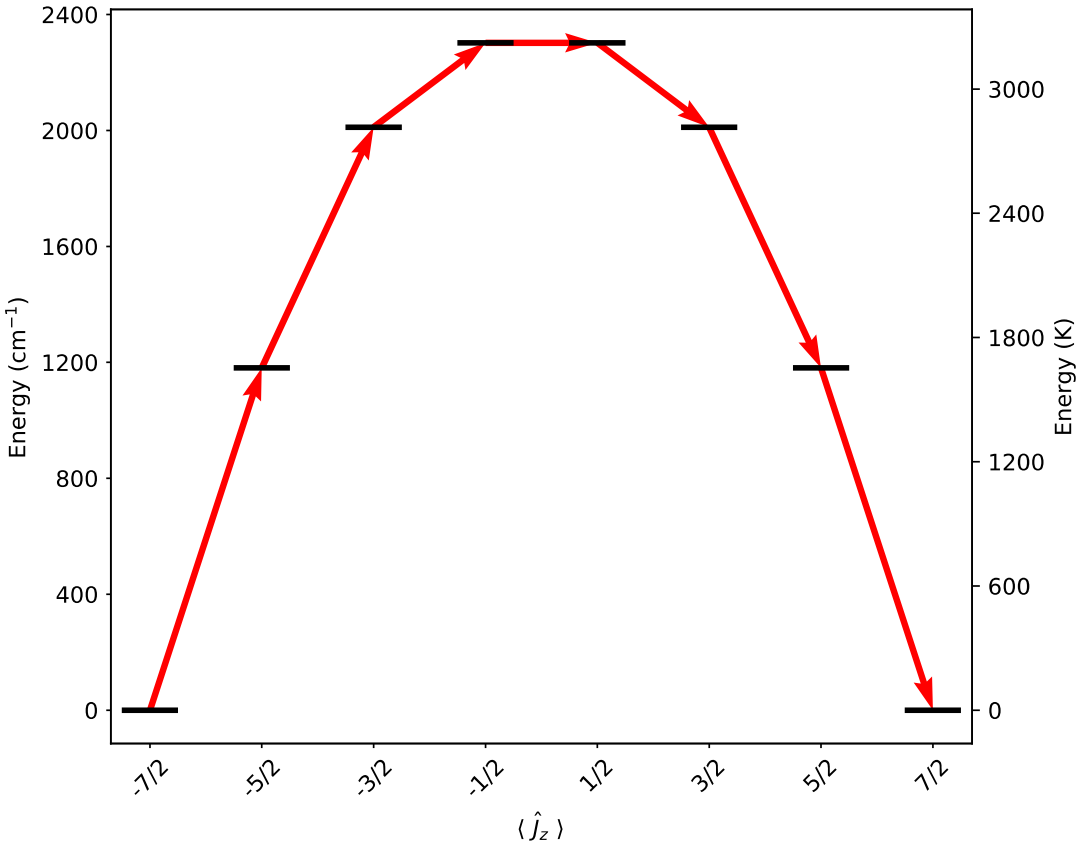

Table S12. Crystal field properties resulted from CASSCF-SO calculations for an idealised YbF_8 molecule in D_{4d} point group symmetry with a Z-displacement of 0.5 Å and plane angles of 73.8° and GS τ_{QTM} = 6448 s.

Crystal field		***g*-tensor values**			**Angle**	**Wavefunction decomposition**
Energy (cm^{-1})	**Energy (K)**	**g_x**	**g_y**	**g_z**	(°)	
0	0	2.10×10^{-6}	2.10×10^{-6}	7.96	--	100%$\vert \pm 7/2\rangle$
1181	1700	4.86×10^{-6}	8.93×10^{-6}	5.61	0	100%$\vert \pm 5/2\rangle$
2011	2894	9.50×10^{-5}	1.10×10^{-4}	3.35	0	100%$\vert \pm 3/2\rangle$
2302	3313	4.56	4.56	1.14	0	100%$\vert \pm 1/2\rangle$

Figure S3. Energy barrier for an idealised YbF_8 molecule in D_{4d} point group symmetry with a Z-displacement of 1.0 Å and plane angles of 61.7°.

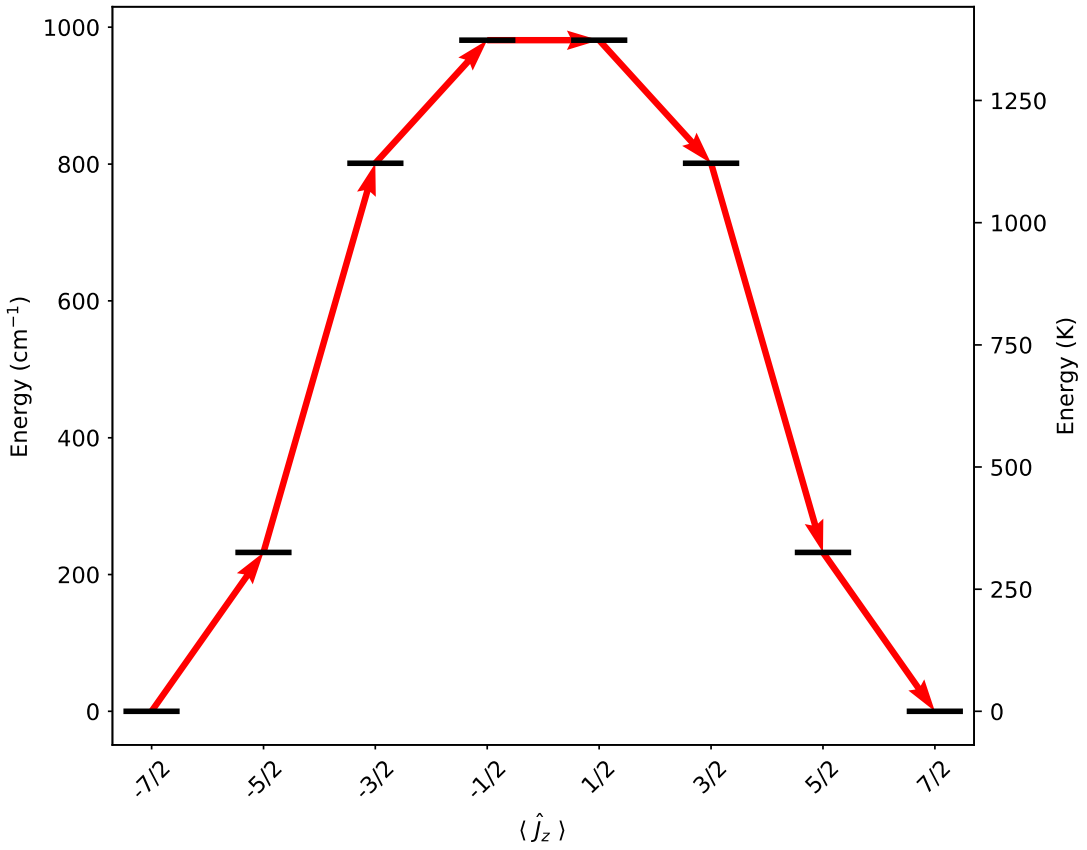

Table S13. Crystal field properties resulted from CASSCF-SO calculations for an idealised YbF_8 molecule in D_{4d} point group symmetry with a Z-displacement of 1.0 Å and plane angles of 61.7° and GS τ_{QTM} = 198 s.

Crystal field		***g*-tensor values**			**Angle**	**Wavefunction**
Energy (cm^{-1})	**Energy (K)**	**g_x**	**g_y**	**g_z**	(°)	**decomposition**
0	0	1.20×10^{-5}	1.20×10^{-5}	7.97	--	100%$\vert \pm 7/2\rangle$
232	334	3.73×10^{-6}	1.99×10^{-5}	5.67	0	100%$\vert \pm 5/2\rangle$
801	1153	2.38×10^{-6}	1.36×10^{-5}	3.35	0	100%$\vert \pm 3/2\rangle$
981	1411	4.56	4.56	1.15	0	100%$\vert \pm 1/2\rangle$

Figure S4. Energy barrier for an idealised YbF_8 molecule in D_{4d} point group symmetry with a Z-displacement of 1.5 Å and plane angles of 44.8°.

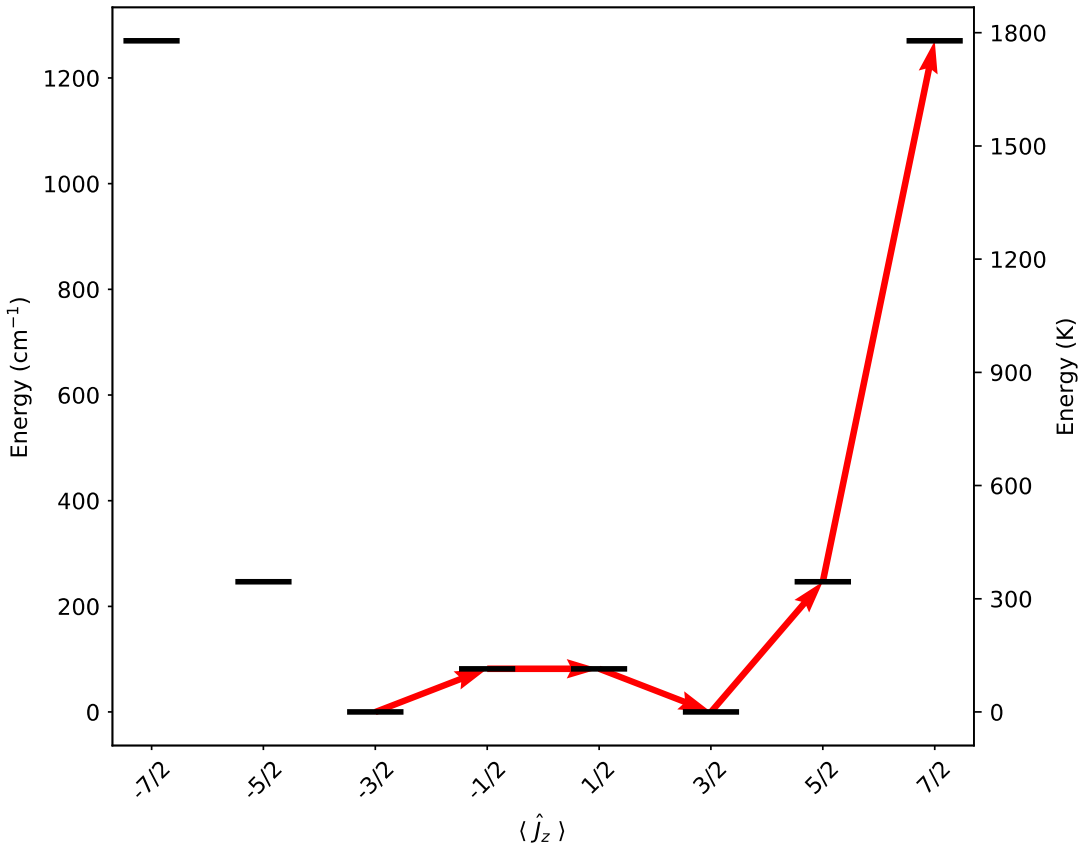

Table S14. Crystal field properties resulted from CASSCF-SO calculations for an idealised YbF_8 molecule in D_{4d} point group symmetry with a Z-displacement of 1.5 Å and plane angles of 44.8°.

Crystal field		***g*-tensor values**			**Angle**	**Wavefunction**
Energy (cm^{-1})	**Energy (K)**	**g_x**	**g_y**	**g_z**	(°)	**decomposition**
0	0	3.80×10^{-6}	2.36×10^{-5}	3.43	--	$100\%\|\pm 3/2\rangle$
82	118	4.55	4.55	1.12	0	$100\%\|\pm 1/2\rangle$
247	355	1.03×10^{-5}	1.75×10^{-5}	5.74	0	$100\%\|\pm 5/2\rangle$
1270	1828	3.25×10^{-6}	3.25×10^{-6}	7.99	0	$100\%\|\pm 7/2\rangle$

Figure S5. Energy barrier for an idealised YbF_8 molecule in D_{4d} point group symmetry with a Z-displacement of 1.1 Å and plane angles of 58.7°.

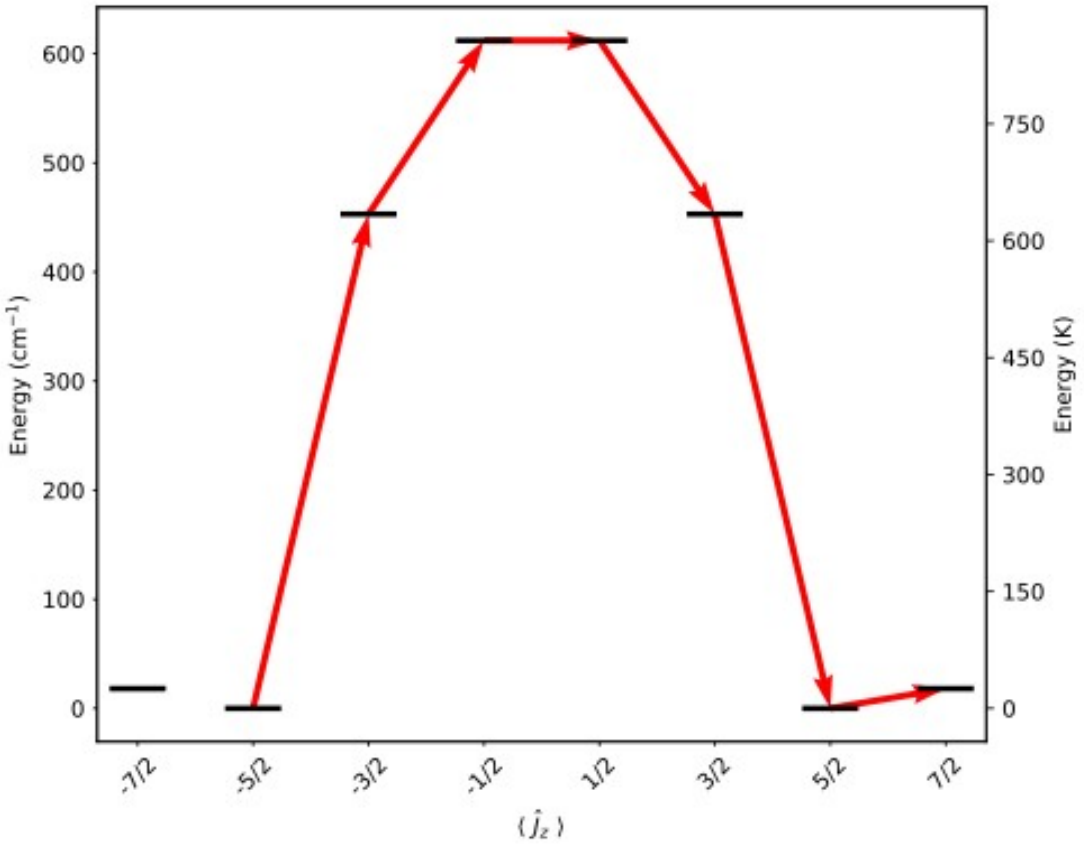

Table S15. Crystal field properties resulted from CASSCF-SO calculations for an idealised YbF_8 molecule in D_{4d} point group symmetry with a Z-displacement of 1.1 Å and plane angles of 58.7°.

Crystal field		***g*-tensor values**			**Angle**	**Wavefunction decomposition**
Energy (cm^{-1})	**Energy (K)**	**g_x**	**g_y**	**g_z**	(°)	
0	0	9.19×10^{-5}	1.16×10^{-4}	5.69	--	100%$\vert \pm 5/2\rangle$
18	26	1.04×10^{-4}	1.04×10^{-4}	7.98	0	100%$\vert \pm 7/2\rangle$
453	652	4.63×10^{-6}	1.98×10^{-5}	3.36	0	100%$\vert \pm 3/2\rangle$
612	881	4.56	4.56	1.15	0	100%$\vert \pm 1/2\rangle$

3. Computational variations

To investigate whether the dramatic underperformance of YbF_x compared to ErF_x could be caused by an overlooked computational parameter, we exchanged various parameters between the different metals. The parameters we investigated was switching the Ln-F bond lengths, exchanging optimised orbitals and swapping basis sets. We also investigated basis set size effects and the addition of CASPT2 to the computational pipeline.

Swapping bond lengths found an overall minor increase in Yb(III) QTM times and a minor decrease in Er(III) QTM times. This can be contextualised as the longer Ln-F bond reduces crystal field interactions with the 4f orbitals that cause wavefunction mixing. However, the change does not significantly affect the several orders of magnitude discrepancy between Er(III) and Yb(III), with results all within an order of magnitude of the original calculations.

In order to swap the optimised orbital, the RasOrb file for the corresponding ErF_x calculation was used with additional of the CIONLY key word for the YbF_x calculation. This ensures that if any errors were generated during a RASSCF optimisation for Yb, they would now be avoided. When the optimised orbitals were swapped between analogous LnF_x compounds, we found a small improvement in Er(III) QTM times and a reduction of Yb(III) QTM times. Again, this can be interpreted since Yb(III) is smaller than the Er(III) ion due to lanthanoid contraction. The basis functions would reflect this and hence the Yb(III) optimised orbitals would be closer to the nucleus and further from the fluoride ions. This would lead to weaker crystal field interactions that could distort the 4f orbitals, minimising the wavefunction mixing found for the $ErF_{x\text{-}orb}$ calculations and increasing QTM times.

For the basis exchange, the ANORCC basis contraction parameters were manually input for the opposite ion, that is Yb basis contractions for the Er calculation and *vice versa*. Exchanging basis sets had a minimal effect on the QTM times. There was a slight reduction of the QTM times of the Er(III) compounds with the Yb(III) basis set and an increase in the Yb(III) QTM times with Er(III) basis set. However, due to the small magnitude of the change, we do not consider it a significant factor in affecting QTM time.

With these variations, we see no change large enough to justify the discrepancy between Er(III) and Yb(III) QTM time as originating from the computational method. This supports our conclusion that Yb(III) has inherently faster QTM times compared to Er(III).

The introduction of CASPT2 had a minor effect on the Yb(III) compounds, with YbF_3 and YbF_5 improving QTM time with CASPT2, while YbF_4 and YbF_6 gave faster QTM time. In the case of Yb(III), CASPT2 does not show a systematic impact on the QTM time. However, for Er(III), the introduction of CASPT2 caused around 10 orders of magnitude reduction in QTM time. Surprisingly ErF_5 has worse computed QTM time than YbF_5 with the introduction of CASPT2. However, aside from Yb(III), CASPT2 is known to provide less accurate description of the ground states of Ln(III) compounds. Hence, we believe that CASPT2 in Er(III) causes erroneous wavefunction mixing, leading to worse QTM times.

Basis Size

Table S16. The comparison of the anisotropy and τ_{QTM} between **Yb_{step}** and **Yb_{equal}** with central ion basis described by VDZP, VTZP or VQZP basis sets.

	Yb_{step}				**Yb_{equal}**			
	g*-tensor *values			**QTM**	***g*-tensor *values***			**QTM**
	g_x	g_y	g_z	(s)	g_x	g_y	g_z	(s)
LnF_3 VDZP	0.247	0.247	7.94	4.65×10^{-7}	0.236	0.236	7.95	5.10×10^{-7}
LnF_3 VTZP	0.213	0.213	7.95	6.26×10^{-7}	0.188	0.188	7.96	8.05×10^{-7}
LnF_3 VQZP	0.180	0.180	7.96	8.78×10^{-7}	0.178	0.178	7.96	8.98×10^{-7}

CASPT2

Table S17. Crystal field properties resulted from CASPT2 calculations for an YbF_3 molecule in D_{3h} point group symmetry.

Crystal field		***g*-tensor values**			**Angle**	**Wavefunction decomposition**
Energy (cm^{-1})	**Energy (K)**	g_x	g_y	g_z	(°)	
0	0	0.213	0.213	7.95	--	99.95%$\lvert \pm 7/2\rangle$; 0.05% $\lvert \mp 5/2\rangle$
1312	1888	0.204	0.204	5.63	0	99.95%$\lvert \pm 5/2\rangle$; 0.05% $\lvert \mp 7/2\rangle$
1822	2621	2.12×10^{-6}	1.49×10^{-5}	3.39	0	100%$\lvert \pm 3/2\rangle$
2109	3035	4.55	4.55	1.12	0	100%$\lvert \pm 1/2\rangle$

Table S18. Crystal field properties resulted from CASPT2 calculations for an YbF_4 molecule in D_{4h} point group symmetry.

Crystal field		***g*-tensor values**			**Angle**	**Wavefunction decomposition**
Energy (cm^{-1})	**Energy (K)**	g_x	g_y	g_z	(°)	
0	0	5.50×10^{-2}	5.50×10^{-2}	7.83	--	98.7%$\lvert \pm 7/2\rangle$; 1.3% $\lvert \mp 1/2\rangle$
1748	2515	2.75	2.75	4.28	0	85.6%$\lvert \pm 5/2\rangle$; 14.4% $\lvert \mp 3/2\rangle$
2774	3991	2.78	2.78	2.09	0	85.6%$\lvert \pm 3/2\rangle$; 14.4% $\lvert \mp 5/2\rangle$
3083	4436	4.49	4.49	0.983	0	98.7%$\lvert \pm 1/2\rangle$; 1.3% $\lvert \mp 7/2\rangle$

Table S19. Crystal field properties resulted from CASPT2 calculations for an YbF_5 molecule in D_{5h} point group symmetry.

Crystal field		***g*-tensor values**			**Angle**	**Wavefunction decomposition**
Energy (cm^{-1})	**Energy (K)**	g_x	g_y	g_z	(°)	
0	0	1.58×10^{-6}	2.95×10^{-6}	7.96	--	100%$\vert \pm 7/2\rangle$
2049	2948	1.34×10^{-2}	1.34×10^{-2}	5.55	0	100%$\vert \pm 5/2\rangle$
2963	4264	1.39×10^{-2}	1.39×10^{-2}	3.37	0	100%$\vert \pm 3/2\rangle$
3457	4974	4.54	4.53	1.09	0	100%$\vert \pm 1/2\rangle$

Table S20. Crystal field properties resulted from CASPT2 calculations for an YbF_6 molecule in D_{6h} point group symmetry.

Crystal field		***g*-tensor values**			**Angle**	**Wavefunction decomposition**
Energy (cm^{-1})	**Energy (K)**	g_x	g_y	g_z	(°)	
0	0	1.17	1.17	7.48	--	97.0%$\vert \pm 7/2\rangle$; 3.0% $\vert \mp 5/2\rangle$
2703	3888	1.08	1.10	5.11	0	97.0%$\vert \pm 5/2\rangle$; 3.0% $\vert \mp 7/2\rangle$
3772	5427	1.16×10^{-2}	1.23×10^{-2}	3.35	0	100%$\vert \pm 3/2\rangle$
4356	6267	4.53	4.53	1.09	0	100%$\vert \pm 1/2\rangle$

Table S21. The comparison of the anisotropy and τ_{QTM} between **Yb_{bond}** and **Er_{bond}** structures with exchange in bond lengths.

	Yb_{bond}				**Er_{bond}**			
	***g*-tensor values**			**QTM**	***g*-tensor values**			**QTM**
	g_x	g_y	g_z	(s)	g_x	g_y	g_z	(s)
LnF_3	0.207	0.207	7.96	6.62×10^{-7}	2.33×10^{-8}	3.83×10^{-8}	17.91	6.36×10^{7}
LnF_4	2.66×10^{-2}	2.66×10^{-2}	7.90	3.98×10^{-5}	1.15×10^{-2}	1.15×10^{-2}	17.79	4.83×10^{-4}
LnF_5	2.62×10^{-6}	2.62×10^{-6}	7.96	4130	2.26×10^{-9}	2.41×10^{-9}	17.89	1.17×10^{10}
LnF_6	0.774	0.774	7.75	4.67×10^{-8}	1.29×10^{-6}	3.74×10^{-6}	17.76	8107

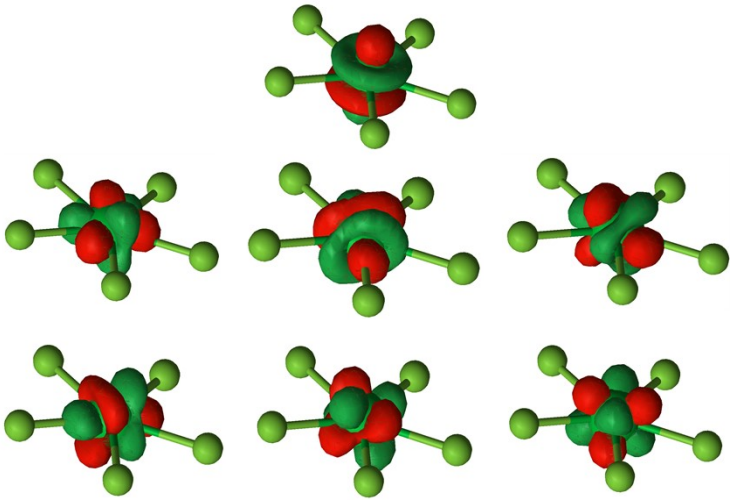

Figure S6. The different optimised active space orbitals shown for YbF_5 clearly indicating the 4f orbitals as the active space.

Table S22. The comparison of the anisotropy and τ_{QTM} between Yb(III) and Er(III) structures with exchange in optimised orbital definitions.

	Yb_{orb}				**Er_{orb}**			
	g*-tensor *values			**QTM**	***g*-tensor *values***			**QTM**
	g_x	g_y	g_z	(s)	g_x	g_y	g_z	(s)
LnF_3	0.379	0.379	7.92	1.97×10^{-7}	2.24×10^{-8}	4.34×10^{-8}	17.91	5.37×10^{7}
LnF_4	5.22×10^{-2}	5.22×10^{-2}	7.84	1.03×10^{-5}	3.00×10^{-3}	3.00×10^{-3}	17.85	7.09×10^{-3}
LnF_5	3.11×10^{-6}	3.11×10^{-6}	7.95	2936	7.52×10^{-11}	9.02×10^{-11}	17.90	9.27×10^{12}
LnF_6	0.918	0.918	7.66	3.29×10^{-8}	1.85×10^{-6}	2.39×10^{-6}	17.83	1.39×10^{4}

Table S23. The comparison of the anisotropy and τ_{QTM} between **Yb_{basis}** and **Er_{basis}** structures with exchange in basis sets.

	Yb_{basis}				**Er_{basis}**			
	g*-tensor *values			**QTM**	***g*-tensor *values***			**QTM**
	g_x	g_y	g_z	(s)	g_x	g_y	g_z	(s)
LnF_3	0.188	0.188	7.96	8.09×10^{-7}	5.85×10^{-8}	5.97×10^{-8}	17.91	1.83×10^{7}
LnF_4	2.33×10^{-2}	2.33×10^{-2}	7.90	5.19×10^{-5}	1.87×10^{-2}	1.87×10^{-2}	17.74	1.82×10^{-4}
LnF_5	1.04×10^{-6}	1.04×10^{-6}	7.95	2.64×10^{4}	4.37×10^{-10}	7.41×10^{-10}	17.90	1.73×10^{11}
LnF_6	0.764	0.764	7.75	4.79×10^{-8}	1.90×10^{-6}	2.20×10^{-6}	17.76	1.51×10^{4}

Bond length swap

Table S24. Crystal field properties resulted from CASSCF-SO calculations for an YbF_3 molecule in D_{3h} point group symmetry using the bond lengths of Er(III)-F.

Crystal field		***g*-tensor values**			**Angle**	**Wavefunction decomposition**
Energy (cm^{-1})	**Energy (K)**	g_x	g_y	g_z	(°)	
0	0	0.207	0.207	7.96	--	99.9%$\lvert \pm 7/2\rangle$; 0.1% $\lvert \mp 5/2\rangle$
979	1409	0.199	0.199	5.63	0	99.9%$\lvert \pm 5/2\rangle$; 0.1% $\lvert \mp 7/2\rangle$
1451	2088	3.30×10^{-6}	1.38×10^{-5}	3.39	0	100%$\lvert \pm 3/2\rangle$
1703	2450	4.55	4.55	1.12	0	100%$\lvert \pm 1/2\rangle$

Table S25. Crystal field properties resulted from CASSCF-SO calculations for an ErF_3 molecule in D_{3h} point group symmetry using the bond lengths of Yb(III)-F.

Crystal field		***g*-tensor values**			**Angle**	**Wavefunction decomposition**
Energy (cm^{-1})	**Energy (K)**	g_x	g_y	g_z	(°)	
0	0	2.33×10^{-8}	3.83×10^{-8}	17.91	--	100%$\lvert \pm 15/2\rangle$
185	266	2.57×10^{-1}	2.57×10^{-1}	15.46	0	99.8%$\lvert \pm 13/2\rangle$; 0.2% $\lvert \pm 1/2\rangle$
260	374	2.25×10^{-1}	2.25×10^{-1}	13.02	0	99.4%$\lvert \pm 11/2\rangle$; 0.6% $\lvert \mp 1/2\rangle$
329	474	3.17×10^{-6}	4.37×10^{-6}	10.45	0	98.1%$\lvert \pm 9/2\rangle$; 1.9% $\lvert \mp 3/2\rangle$
418	601	5.86	5.86	6.56	0	87.6%$\lvert \pm 7/2\rangle$; 12.4% $\lvert \mp 5/2\rangle$
575	827	5.85	5.85	4.16	0	87.6%$\lvert \pm 5/2\rangle$; 12.4% $\lvert \mp 7/2\rangle$
668	961	1.76×10^{-5}	2.71×10^{-5}	3.27	0	98.1%$\lvert \pm 3/2\rangle$; 1.9% $\lvert \mp 9/2\rangle$
727	1046	9.52	9.52	1.12	0	99.2%$\lvert \pm 1/2\rangle$; 0.6% $\lvert \mp 11/2\rangle$; 0.2%$\lvert \pm 13/2\rangle$

Table S26. Crystal field properties resulted from CASSCF-SO calculations for an YbF_4 molecule in D_{4h} point group symmetry using the bond lengths of Er(III)-F.

Crystal field		***g*-tensor values**			**Angle**	**Wavefunction decomposition**
Energy (cm^{-1})	**Energy (K)**	g_x	g_y	g_z	(°)	
0	0	2.66×10^{-2}	2.66×10^{-2}	7.90	--	99.4%$\lvert \pm 7/2\rangle$; 0.6% $\lvert \mp 1/2\rangle$
1316	1893	1.96	1.96	5.01	0	93.3%$\lvert \pm 5/2\rangle$; 6.7% $\lvert \mp 3/2\rangle$
2051	2951	1.98	1.98	2.78	0	93.3%$\lvert \pm 3/2\rangle$; 6.7% $\lvert \mp 5/2\rangle$
2366	3404	4.52	4.52	1.05	0	99.4%$\lvert \pm 1/2\rangle$; 0.6% $\lvert \mp 7/2\rangle$

Table S27. Crystal field properties resulted from CASSCF-SO calculations for an ErF_4 molecule in D_{4h} point group symmetry using the bond lengths of Yb(III)-F.

Crystal field		***g*-tensor values**			**Angle**	**Wavefunction decomposition**
Energy (cm^{-1})	**Energy (K)**	g_x	g_y	g_z	(°)	
0	0	1.15×10^{-2}	1.15×10^{-2}	17.79	--	98.8%$\|\pm 15/2\rangle$; 1.2%$\|\pm 7/2\rangle$
285	410	2.56×10^{-2}	2.56×10^{-2}	15.33	0	98.7%$\|\pm 13/2\rangle$; 1.1%$\|\pm 5/2\rangle$; 0.2%$\|\mp 3/2\rangle$
384	552	0.210	0.210	13.05	0	99.5%$\|\pm 11/2\rangle$; 0.3%$\|\pm 3/2\rangle$; 0.1% $\|\mp 5/2\rangle$
439	631	5.05	5.05	8.44	0	84.1%$\|\pm 9/2\rangle$; 8.5% $\|\mp 7/2\rangle$; 7.2%$\|\pm 1/2\rangle$; 0.2% $\|\mp 15/2\rangle$
552	795	4.58	4.58	5.22	0	78.2%$\|\pm 7/2\rangle$; 13.4% $\|\mp 9/2\rangle$; 7.4% $\|\mp 1/2\rangle$; 1.0%$\|\pm 15/2\rangle$;
605	871	8.63	8.63	2.72	0	64.3%$\|\pm 5/2\rangle$; 34.1% $\|\mp 3/2\rangle$; 1.2%$\|\pm 13/2\rangle$; 0.4% $\|\mp 11/2\rangle$
1121	1613	8.79	8.79	0.255	0	65.4%$\|\pm 3/2\rangle$; 34.5% $\|\mp 5/2\rangle$; 0.1% $\|\mp 13/2\rangle$
1131	1627	9.06	9.06	0.256	0	85.3%$\|\pm 1/2\rangle$; 12.1% $\|\mp 7/2\rangle$; 2.5%$\|\pm 13/2\rangle$

Table S28. Crystal field properties resulted from CASSCF-SO calculations for an YbF_5 molecule in D_{5h} point group symmetry using the bond lengths of Er(III)-F.

Crystal field		***g*-tensor values**			**Angle**	**Wavefunction decomposition**
Energy (cm^{-1})	**Energy (K)**	g_x	g_y	g_z	(°)	
0	0	2.62×10^{-6}	2.62×10^{-6}	7.96	--	100%$\vert \pm 7/2\rangle$
1554	2236	1.52×10^{-6}	6.47×10^{-6}	5.59	0	100%$\vert \pm 5/2\rangle$
2329	3351	1.55×10^{-6}	6.33×10^{-6}	3.37	0	100%$\vert \pm 3/2\rangle$
2748	3954	4.54	4.54	1.11	0	100%$\vert \pm 1/2\rangle$

Table S29. Crystal field properties resulted from CASSCF-SO calculations for an ErF_5 molecule in D_{5h} point group symmetry using the bond lengths of Yb(III)-F.

Crystal field		***g*-tensor values**			**Angle**	**Wavefunction decomposition**
Energy (cm^{-1})	**Energy (K)**	g_x	g_y	g_z	(°)	
0	0	2.26×10^{-9}	2.41×10^{-9}	17.89	--	100%$\vert \pm 15/2\rangle$
339	487	5.33×10^{-9}	6.59×10^{-9}	15.46	0	100%$\vert \pm 13/2\rangle$
459	661	2.00×10^{-2}	2.00×10^{-2}	13.10	0	100%$\vert \pm 11/2\rangle$
563	810	1.99×10^{-2}	1.99×10^{-2}	10.70	0	100%$\vert \pm 9/2\rangle$
718	1033	2.94×10^{-5}	3.45×10^{-5}	8.28	0	100%$\vert \pm 7/2\rangle$
907	1305	3.30×10^{-5}	9.68×10^{-5}	5.87	0	100%$\vert \pm 5/2\rangle$
1081	1556	5.99×10^{-5}	6.98×10^{-5}	3.50	0	100%$\vert \pm 3/2\rangle$
1186	1706	9.53	9.53	1.16	0	100%$\vert \pm 1/2\rangle$

Table S30. Crystal field properties resulted from CASSCF-SO calculations for an YbF_6 molecule in D_{6h} point group symmetry using the bond lengths of Er(III)-F.

Crystal field		***g*-tensor values**			**Angle**	**Wavefunction decomposition**
Energy (cm^{-1})	**Energy (K)**	**g_x**	**g_y**	**g_z**	(°)	
0	0	0.774	0.774	7.75	--	98.7%$\vert \pm 7/2\rangle$; 1.3% $\vert \mp 5/2\rangle$
1918	2760	0.728	0.728	5.39	0	98.7%$\vert \pm 5/2\rangle$; 1.3% $\vert \mp 7/2\rangle$
2828	4069	4.01×10^{-6}	5.23×10^{-6}	3.36	0	100%$\vert \pm 3/2\rangle$
3315	4770	4.54	4.54	1.10	0	100%$\vert \pm 1/2\rangle$

Table S31. Crystal field properties resulted from CASSCF-SO calculations for an ErF_6 molecule in D_{6h} point group symmetry using the bond lengths of Yb(III)-F.

Crystal field		***g*-tensor values**			**Angle**	**Wavefunction decomposition**
Energy (cm^{-1})	**Energy (K)**	**g_x**	**g_y**	**g_z**	(°)	
0	0	1.29×10^{-6}	3.74×10^{-6}	17.76	--	99.3%$\vert \pm 15/2\rangle$; 0.6%$\vert \pm 3/2\rangle$; 0.1%$\vert \mp 9/2\rangle$
347	499	4.14	4.14	11.96	0	85.0%$\vert \pm 13/2\rangle$; 5.5%$\vert \pm 1/2\rangle$; 9.4%$\vert \mp 11/2\rangle$
476	686	3.75	3.75	8.89	90	83.3%$\vert \mp 11/2\rangle$; 4.0 %$\vert \pm 1/2\rangle$; 12.6%$\vert \pm 11/2\rangle$
512	737	1.20×10^{-4}	1.62×10^{-4}	8.17	0	82.8%$\vert \mp 9/2\rangle$; 16.8%$\vert \pm 3/2\rangle$; 0.4% $\vert \pm 15/2\rangle$
558	802	8.59	8.59	3.09	0	63.5%$\vert \pm 7/2\rangle$; 36.5%$\vert \mp 5/2\rangle$
1412	2031	8.53	8.53	0.696	0	63.5%$\vert \mp 5/2\rangle$; 36.5%$\vert \pm 7/2\rangle$
1478	2127	1.22×10^{-4}	3.56×10^{-4}	1.11	0	82.6%$\vert \pm 3/2\rangle$; 17.1%$\vert \mp 9/2\rangle$; 0.3%$\vert \pm 15/2\rangle$;
1541	2218	9.13	9.13	0.460	0	90.4%$\vert \pm 1/2\rangle$; 7.2%$\vert \mp 11/2\rangle$; 2.3%$\vert \pm 13/2\rangle$

Optimised orbital exchange

Table S32. Crystal field properties resulted from CASSCF-SO calculations for an YbF_3 molecule in D_{3h} point group symmetry using the optimised orbital definitions of Er(III)-F.

Crystal field		***g*-tensor values**			**Angle**	**Wavefunction decomposition**
Energy (cm^{-1})	**Energy (K)**	g_x	g_y	g_z	(°)	
0	0	0.379	0.379	7.92	--	99.7%$\vert \pm 7/2\rangle$; 0.3%$\vert \mp 5/2\rangle$
876	1260	0.363	0.363	5.60	0	99.7%$\vert \pm 5/2\rangle$; 0.3% $\vert \mp 7/2\rangle$
1219	1753	4.67×10^{-6}	2.38×10^{-5}	3.40	0	100%$\vert \pm 3/2\rangle$
1421	2044	4.55	4.55	1.12	0	100%$\vert \pm 1/2\rangle$

Table S33. Crystal field properties resulted from CASSCF-SO calculations for an ErF_3 molecule in D_{3h} point group symmetry using the optimised orbital definitions of Yb(III)-F.

Crystal field		***g*-tensor values**			**Angle**	**Wavefunction decomposition**
Energy (cm^{-1})	**Energy (K)**	**g_x**	**g_y**	**g_z**	(°)	
0	0	2.24×10^{-8}	4.34×10^{-8}	17.91	--	100%$\lvert \pm 15/2\rangle$
226	325	0.109	0.109	15.48	0	99.9%$\lvert \pm 13/2\rangle$; 0.1% $\lvert \pm 1/2\rangle$
342	492	8.98×10^{-2}	8.98×10^{-2}	13.06	0	99.6%$\lvert \pm 11/2\rangle$; 0.4% $\lvert \mp 1/2\rangle$
442	636	4.26×10^{-6}	1.04×10^{-5}	10.54	0	98.8%$\lvert \pm 9/2\rangle$; 1.2% $\lvert \mp 3/2\rangle$
551	793	5.17	5.17	6.99	0	90.9%$\lvert \pm 7/2\rangle$; 9.1% $\lvert \mp 5/2\rangle$
707	1017	5.16	5.16	4.59	0	90.9%$\lvert \pm 5/2\rangle$; 9.1% $\lvert \mp 7/2\rangle$
805	1159	9.45×10^{-6}	1.43×10^{-4}	3.36	0	98.8%$\lvert \pm 3/2\rangle$; 1.2% $\lvert \mp 9/2\rangle$
866	1246	9.53	9.53	1.14	0	99.5%$\lvert \pm 1/2\rangle$; 0.4% $\lvert \mp 11/2\rangle$; 0.1%$\lvert \pm 13/2\rangle$

Table S34. Crystal field properties resulted from CASSCF-SO calculations for an YbF_4 molecule in D_{4h} point group symmetry using the optimised orbital definitions of Er(III)-F.

Crystal field		***g*-tensor values**			**Angle**	**Wavefunction decomposition**
Energy (cm^{-1})	**Energy (K)**	g_x	g_y	g_z	(°)	
0	0	5.22×10^{-2}	5.22×10^{-2}	7.84	--	98.8%$\lvert \pm 7/2\rangle$; 1.2% $\lvert \mp 1/2\rangle$
1111	1599	2.63	2.63	4.47	0	87.2%$\lvert \pm 5/2\rangle$; 12.8% $\lvert \mp 3/2\rangle$
1726	2484	2.23	2.65	2.65	0	87.2%$\lvert \pm 3/2\rangle$; 12.8% $\lvert \mp 5/2\rangle$
1941	2793	4.50	4.50	1.00	0	98.8%$\lvert \pm 1/2\rangle$; 1.2% $\lvert \mp 7/2\rangle$

Table S35. Crystal field properties resulted from CASSCF-SO calculations for an ErF_4 molecule in D_{4h} point group symmetry using the optimised orbital definitions of Yb(III)-F.

Crystal field		***g*-tensor values**			**Angle**	**Wavefunction decomposition**
Energy (cm^{-1})	**Energy (K)**	g_x	g_y	g_z	(°)	
0	0	3.00×10^{-3}	3.00×10^{-3}	17.85	--	99.4%$\lvert \pm 15/2\rangle$; 0.6%$\lvert \pm 7/2\rangle$
327	470	5.60×10^{-3}	5.60×10^{-3}	15.42	0	99.5%$\lvert \pm 13/2\rangle$; 0.5%$\lvert \pm 5/2\rangle$
475	683	6.97×10^{-2}	6.97×10^{-2}	13.08	0	99.8%$\lvert \pm 11/2\rangle$; 0.2%$\lvert \pm 3/2\rangle$
577	831	3.53	3.53	9.54	0	91.3%$\lvert \pm 9/2\rangle$; 4.7%$\lvert \pm 1/2\rangle$; 4.0% $\lvert \mp 7/2\rangle$
707	1017	3.11	3.11	6.38	0	84.9%$\lvert \pm 7/2\rangle$; 7.9% $\lvert \mp 1/2\rangle$; 6.7% $\lvert \mp 9/2\rangle$; 0.5%$\lvert \pm 15/2\rangle$
783	1127	2.81	8.65	8.65	90	66.5%$\lvert \pm 5/2\rangle$; 32.8% $\lvert \mp 3/2\rangle$; 0.5%$\lvert \pm 13/2\rangle$; 0.2% $\lvert \mp 11/2\rangle$
1247	1794	0.405	8.70	8.70	90	67%$\lvert \pm 3/2\rangle$; 32.9%$\lvert \mp 5/2\rangle$; 0.1%$\lvert \mp 13/2\rangle$
1262	1815	0.369	9.12	9.12	90	87.5%$\lvert \pm 1/2\rangle$; 10.5% $\lvert \mp 7/2\rangle$; 2.0%$\lvert \pm 9/2\rangle$

Table S36. Crystal field properties resulted from CASSCF-SO calculations for an YbF_5 molecule in D_{5h} point group symmetry using the optimised orbital definitions of Er(III)-F.

Crystal field		***g*-tensor values**			**Angle**	**Wavefunction decomposition**
Energy (cm^{-1})	**Energy (K)**	g_x	g_y	g_z	(°)	
0	0	3.11×10^{-6}	3.11×10^{-6}	7.95	--	100%$\vert \pm 7/2\rangle$
1351	1944	3.63×10^{-6}	9.48×10^{-6}	5.61	0	100%$\vert \pm 5/2\rangle$
1928	2774	7.85×10^{-7}	1.21×10^{-5}	3.39	0	100%$\vert \pm 3/2\rangle$
2257	3248	4.54	4.54	1.11	0	100%$\vert \pm 1/2\rangle$

Table S37. Crystal field properties resulted from CASSCF-SO calculations for an ErF_5 molecule in D_{5h} point group symmetry using the optimised orbital definitions of Yb(III)-F.

Crystal field		***g*-tensor values**			**Angle**	**Wavefunction decomposition**
Energy (cm^{-1})	**Energy (K)**	g_x	g_y	g_z	(°)	
0	0	7.52×10^{-11}	9.02×10^{-11}	17.90	--	100%$\vert \pm 15/2\rangle$
382	549	5.06×10^{-9}	5.34×10^{-9}	15.46	0	100%$\vert \pm 13/2\rangle$
554	797	1.10×10^{-3}	1.10×10^{-3}	13.09	0	100%$\vert \pm 11/2\rangle$
698	1004	1.10×10^{-3}	1.10×10^{-3}	10.69	0	100%$\vert \pm 9/2\rangle$
875	1259	5.82×10^{-5}	5.93×10^{-5}	8.28	0	100%$\vert \pm 7/2\rangle$
1073	1543	5.09×10^{-5}	6.64×10^{-5}	5.87	0	100%$\vert \pm 5/2\rangle$
1247	1794	2.51×10^{-5}	4.06×10^{-5}	3.50	0	100%$\vert \pm 3/2\rangle$
1349	1941	9.54	9.54	1.16	0	100%$\vert \pm 1/2\rangle$

Table S38. Crystal field properties resulted from CASSCF-SO calculations for an YbF_6 molecule in D_{6h} point group symmetry using the optimised orbital definitions of Er(III)-F.

Crystal field		***g*-tensor values**			**Angle**	**Wavefunction decomposition**
Energy (cm^{-1})	**Energy (K)**	g_x	g_y	g_z	(°)	
0	0	0.918	0.918	7.66	--	98.1%$\lvert \pm 7/2\rangle$; 1.9% $\lvert \mp 5/2\rangle$
1691	2433	0.864	0.864	5.33	0	98.1%$\lvert \pm 5/2\rangle$; 1.9% $\lvert \mp 7/2\rangle$
2367	3406	9.15×10^{-7}	1.01×10^{-5}	3.38	0	100%$\lvert \pm 3/2\rangle$
2756	3966	4.54	4.54	1.10	0	100%$\lvert \pm 1/2\rangle$

Table S39. Crystal field properties resulted from CASSCF-SO calculations for an ErF_6 molecule in D_{6h} point group symmetry using the optimised orbital definitions of Yb(III)-F.

Crystal field		***g*-tensor values**			**Angle**	**Wavefunction decomposition**
Energy (cm^{-1})	**Energy (K)**	**g_x**	**g_y**	**g_z**	(°)	
0	0	1.85×10^{-6}	2.39×10^{-6}	17.83	--	99.7%$\lvert \pm 15/2\rangle$; 0.3%$\lvert \pm 3/2\rangle$;
407	586	2.32	2.32	14.25	0	94.6%$\lvert \pm 13/2\rangle$; 2.7%$\lvert \mp 11/2\rangle$; 2.9%$\lvert \pm 1/2\rangle$
579	834	2.02	2.02	11.31	0	91.7%$\lvert \pm 11/2\rangle$; 4.0%$\lvert \mp 13/2\rangle$; 4.4%$\lvert \mp 1/2\rangle$
672	967	8.59×10^{-5}	1.13×10^{-4}	8.57	0	85.4%$\lvert \pm 9/2\rangle$; 14.5%$\lvert \mp 3/2\rangle$; 0.15%$\lvert \mp 15/2\rangle$
747	1075	8.50	8.50	3.33	0	65.4%$\lvert \pm 7/2\rangle$; 34.6%$\lvert \mp 5/2\rangle$
1512	2175	8.45	8.45	0.935	0	65.4%$\lvert \pm 5/2\rangle$; 34.6%$\lvert \mp 7/2\rangle$
1585	2281	2.67×10^{-5}	5.59×10^{-5}	1.46	0	85.2%$\lvert \pm 3/2\rangle$; 14.6%$\lvert \mp 9/2\rangle$; 0.2%$\lvert \pm 15/2\rangle$
1651	2375	9.22	9.22	0.596	0	92.7%$\lvert \pm 1/2\rangle$; 5.6%$\lvert \mp 11/2\rangle$; 1.7%$\lvert \pm 13/2\rangle$

Basis set exchange

Table S40. Crystal field properties resulted from CASSCF-SO calculations for an YbF_3 molecule in D_{3h} point group symmetry using the basis set of Er(III).

Crystal field		***g*-tensor values**			**Angle**	**Wavefunction decomposition**
Energy (cm^{-1})	**Energy (K)**	g_x	g_y	g_z	(°)	
0	0	0.188	0.188	7.96	--	99.9%$\lvert \pm 7/2\rangle$; 0.1% $\lvert \mp 5/2\rangle$
999	1438	0.180	0.180	5.63	0	99.9%$\lvert \pm 5/2\rangle$; 0.1% $\lvert \mp 7/2\rangle$
1491	2146	3.66×10^{-6}	4.01×10^{-6}	3.39	0	100%$\lvert \pm 3/2\rangle$
1756	2527	4.56	4.55	1.12	0	100%$\lvert \pm 1/2\rangle$

Table S41. Crystal field properties resulted from CASSCF-SO calculations for an ErF_3 molecule in D_{3h} point group symmetry using the basis set of Yb(III).

Crystal field		***g*-tensor values**			**Angle**	**Wavefunction decomposition**
Energy (cm^{-1})	**Energy (K)**	**g_x**	**g_y**	**g_z**	(°)	
0	0	5.85×10^{-8}	5.97×10^{-8}	17.91	--	99.9%$\vert \pm 15/2\rangle$; 0.1% $\vert \pm 3/2\rangle$
177	255	0.535	0.535	15.41	0	99.4%$\vert \pm 13/2\rangle$; 0.4%$\vert \pm 1/2\rangle$; 0.2%$\vert \mp 11/2\rangle$
236	340	0.481	0.481	12.93	0	98.9%$\vert \pm 11/2\rangle$; 0.9% $\vert \mp 1/2\rangle$; 0.2%$\vert \mp 13/2\rangle$
289	416	7.80×10^{-6}	1.75×10^{-5}	10.30	0	97.0%$\vert \pm 9/2\rangle$; 3.0% $\vert \mp 3/2\rangle$
362	521	6.62	6.62	5.96	0	83.4%$\vert \pm 7/2\rangle$; 16.6% $\vert \mp 5/2\rangle$
532	766	6.61	6.61	3.56	0	83.4%$\vert \pm 5/2\rangle$; 16.6% $\vert \mp 7/2\rangle$
619	890	3.50×10^{-5}	1.60×10^{-4}	3.11	0	97.0%$\vert \pm 3/2\rangle$; 3.0% $\vert \mp 9/2\rangle$
677	974	9.50	9.50	1.08	0	98.7%$\vert \pm 1/2\rangle$; 1% $\vert \mp 11/2\rangle$; 0.3%$\vert \pm 13/2\rangle$

Table S42. Crystal field properties resulted from CASSCF-SO calculations for an YbF_4 molecule in D_{4h} point group symmetry using the basis set of Er(III).

Crystal field		***g*-tensor values**			**Angle**	**Wavefunction decomposition**
Energy (cm^{-1})	**Energy (K)**	**g_x**	**g_y**	**g_z**	(°)	
0	0	2.33×10^{-2}	2.33×10^{-2}	7.90	--	99.4%$\vert \pm 7/2\rangle$; 0.6% $\vert \mp 1/2\rangle$
1372	1973	1.81	1.81	5.10	0	94.3%$\vert \pm 5/2\rangle$; 5.7% $\vert \mp 3/2\rangle$
2140	3079	1.84	1.84	2.87	0	94.3%$\vert \pm 3/2\rangle$; 5.7% $\vert \mp 5/2\rangle$
2486	3576	4.52	4.52	1.06	0	99.4%$\vert \pm 1/2\rangle$; 0.6% $\vert \mp 7/2\rangle$

Table S43. Crystal field properties resulted from CASSCF-SO calculations for an ErF_4 molecule in D_{4h} point group symmetry using the basis set of Yb(III).

Crystal field		***g*-tensor values**			**Angle**	**Wavefunction decomposition**
Energy (cm^{-1})	**Energy (K)**	**g_x**	**g_y**	**g_z**	(°)	
0	0	1.87×10^{-2}	1.87×10^{-2}	17.74	--	98.3%$\vert \pm 15/2\rangle$; 1.6%$\vert \pm 7/2\rangle$; 0.1%$\vert \mp 1/2\rangle$
265	382	7.66×10^{-3}	7.66×10^{-3}	15.22	0	97.6%$\vert \pm 13/2\rangle$; 2%$\vert \pm 5/2\rangle$; 0.3%$\vert \mp 3/2\rangle$
343	493	0.271	0.271	13.06	0	99.6%$\vert \pm 11/2\rangle$; 0.3%$\vert \pm 3/2\rangle$; 0.1% $\vert \mp 5/2\rangle$
376	541	5.43	5.43	8.07	0	82.5%$\vert \pm 9/2\rangle$; 9.8% $\vert \mp 7/2\rangle$; 7.4%$\vert \pm 1/2\rangle$; 0.3% $\vert \mp 15/2\rangle$
477	686	4.96	4.96	4.88	0	76.6%$\vert \pm 7/2\rangle$; 15.0% $\vert \mp 9/2\rangle$; 7.2% $\vert \mp 1/2\rangle$; 1.3%$\vert \pm 15/2\rangle$;
521	749	8.54	8.54	2.81	0	63.2%$\vert \pm 5/2\rangle$; 34.3% $\vert \mp 3/2\rangle$; 2.2%$\vert \pm 13/2\rangle$; 0.3% $\vert \mp 11/2\rangle$
1013	1457	8.80	8.80	0.226	0	65.1%$\vert \pm 3/2\rangle$; 34.7% $\vert \mp 5/2\rangle$; 0.1% $\vert \mp 13/2\rangle$; 0.1%$\vert \pm 11/2\rangle$;
1022	1470	9.05	9.05	0.237	0	85.3%$\vert \pm 1/2\rangle$; 12.2% $\vert \mp 7/2\rangle$; 2.5%$\vert \pm 13/2\rangle$

Table S44. Crystal field properties resulted from CASSCF-SO calculations for an YbF_5 molecule in D_{5h} point group symmetry using the basis set of Er(III).

Crystal field		***g*-tensor values**			**Angle**	**Wavefunction decomposition**
Energy (cm^{-1})	**Energy (K)**	**g_x**	**g_y**	**g_z**	(°)	
0	0	1.04×10^{-6}	1.04×10^{-6}	7.95	--	100%$\vert \pm 7/2\rangle$
1627	2341	2.63×10^{-7}	2.20×10^{-6}	5.59	0	100%$\vert \pm 5/2\rangle$
2468	3550	5.71×10^{-6}	8.54×10^{-6}	3.36	0	100%$\vert \pm 3/2\rangle$
2920	4202	4.54	4.54	1.10	0	100%$\vert \pm 1/2\rangle$

Table S45. Crystal field properties resulted from CASSCF-SO calculations for an ErF_5 molecule in D_{5h} point group symmetry using the basis set of Yb(III).

Crystal field		***g*-tensor values**			**Angle**	**Wavefunction decomposition**
Energy (cm^{-1})	**Energy (K)**	**g_x**	**g_y**	**g_z**	(°)	
0	0	4.37×10^{-10}	7.41×10^{-10}	17.90	--	100%$\vert \pm 15/2\rangle$
317	456	2.93×10^{-8}	3.13×10^{-8}	15.47	0	100%$\vert \pm 13/2\rangle$
411	592	1.66×10^{-2}	1.66×10^{-2}	13.11	0	100%$\vert \pm 11/2\rangle$
491	707	1.66×10^{-2}	1.66×10^{-2}	10.71	0	100%$\vert \pm 9/2\rangle$
628	903	7.35×10^{-5}	8.94×10^{-5}	8.29	0	100%$\vert \pm 7/2\rangle$
806	1159	7.09×10^{-5}	9.17×10^{-5}	5.88	0	100%$\vert \pm 5/2\rangle$
973	1401	9.65×10^{-6}	1.11×10^{-5}	3.50	0	100%$\vert \pm 3/2\rangle$
1075	1547	9.54	9.54	1.16	0	100%$\vert \pm 1/2\rangle$

Table S46. Crystal field properties resulted from CASSCF-SO calculations for an YbF_6 molecule in D_{6h} point group symmetry using the basis set of Er(III).

Crystal field		***g*-tensor values**			**Angle**	**Wavefunction decomposition**
Energy (cm^{-1})	**Energy (K)**	**g_x**	**g_y**	**g_z**	(°)	
0	0	0.764	0.764	7.75	--	98.7%$\vert \pm 7/2\rangle$; 1.3% $\vert \mp 5/2\rangle$
2019	2905	0.720	0.720	5.38	0	98.7%$\vert \pm 5/2\rangle$; 1.3% $\vert \mp 7/2\rangle$
3016	4339	6.37×10^{-6}	8.52×10^{-6}	3.35	0	100%$\vert \pm 3/2\rangle$
3543	5098	4.54	4.54	1.10	0	100%$\vert \pm 1/2\rangle$

Table S47. Crystal field properties resulted from CASSCF-SO calculations for an ErF_6 molecule in D_{6h} point group symmetry using the basis set of Yb(III).

Crystal field		***g*-tensor values**			**Angle**	**Wavefunction decomposition**
Energy (cm^{-1})	**Energy (K)**	**g_x**	**g_y**	**g_z**	(°)	
0	0	1.90×10^{-6}	2.20×10^{-6}	17.76	--	99.3%$\vert \pm 15/2\rangle$; 0.6%$\vert \pm 3/2\rangle$; 0.1%$\vert \mp 9/2\rangle$
320	460	4.74	4.74	10.80	0	80.6%$\vert \pm 13/2\rangle$; 13.1%$\vert \mp 11/2\rangle$; 6.3%$\vert \pm 1/2\rangle$
427	614	4.35	4.35	7.74	0	79.6%$\vert \pm 11/2\rangle$; 17.0%$\vert \mp 13/2\rangle$; 3.5% $\vert \mp 1/2\rangle$
441	635	1.03×10^{-4}	3.11×10^{-4}	8.20	0	83.0%$\vert \pm 9/2\rangle$; 16.6% $\vert \mp 7/2\rangle$; 0.4% $\vert \mp 15/2\rangle$
477	686	8.58	8.58	3.13	0	63.7%$\vert \pm 7/2\rangle$; 36.3% $\vert \mp 5/2\rangle$
1257	1809	8.52	8.52	0.73	0	63.7%$\vert \pm 5/2\rangle$; 36.3% $\vert \mp 7/2\rangle$
1327	1910	8.14×10^{-5}	8.86×10^{-5}	1.14	0	82.8%$\vert \pm 3/2\rangle$; 16.9% $\vert \mp 9/2\rangle$; 0.3%$\vert \pm 15/2\rangle$
1393	2004	9.13	9.13	0.47	0	90.3%$\vert \pm 1/2\rangle$; 7.3% $\vert \mp 11/2\rangle$; 2.4%$\vert \pm 13/2\rangle$

4. Model Hamiltonian Simulations

Table S48. Crystal field parameters from CASSCF calculations on the YbF_x series with bold parameters indicating truncated point group terms.

CFP	*YbF_3*	*YbF_4*	*YbF_5*	*YbF_6*	*YbF_8*
B_2^{-2}	-1.77 × 10^{-6}	-3.42 × 10^{-6}	4.98 × 10^{-7}	2.15 × 10^{-7}	-1.21 × 10^{-6}
B_2^{-1}	-7.54 × 10^{-8}	-1.30 × 10^{-8}	-8.70 × 10^{-10}	9.76 × 10^{-9}	2.09 × 10^{-6}
B_2^0	**-48.1**	**-66.4**	**-77.9**	**-93.9**	**-28.1**
B_2^1	-1.32 × 10^{-9}	2.83 × 10^{-8}	-4.43 × 10^{-9}	1.71 × 10^{-8}	-2.04 × 10^{-6}
B_2^2	6.96 × 10^{-5}	-3.80 × 10^{-5}	-2.12 × 10^{-6}	4.26 × 10^{-5}	4.40 × 10^{-5}
B_4^{-4}	1.85 × 10^{-7}	2.64 × 10^{-1}	3.41 × 10^{-7}	3.62 × 10^{-7}	1.65 × 10^{-7}
B_4^{-3}	6.93 × 10^{-9}	-4.41 × 10^{-9}	1.21 × 10^{-8}	-8.48 × 10^{-9}	-1.40 × 10^{-7}
B_4^{-2}	4.55 × 10^{-8}	-5.84 × 10^{-8}	-3.12 × 10^{-8}	3.18 × 10^{-8}	2.01 × 10^{-8}
B_4^{-1}	2.98 × 10^{-9}	1.18 × 10^{-10}	-7.81 × 10^{-11}	-1.04 × 10^{-10}	-9.86 × 10^{-8}
B_4^0	**-1.00 × 10^{-1}**	**-1.44 × 10^{-1}**	**-1.41 × 10^{-1}**	**-1.78 × 10^{-1}**	**1.84 × 10^{-1}**
B_4^1	2.90 × 10^{-10}	-6.72 × 10^{-10}	1.69 × 10^{-10}	-1.89 × 10^{-9}	9.53 × 10^{-8}
B_4^2	2.76 × 10^{-6}	-2.69 × 10^{-6}	1.82 × 10^{-6}	5.77 × 10^{-7}	2.28 × 10^{-6}
B_4^3	-1.79 × 10^{-9}	-3.41 × 10^{-9}	1.40 × 10^{-8}	-9.44 × 10^{-9}	1.33 × 10^{-7}
B_4^4	4.87 × 10^{-6}	**-2.18**	-3.61 × 10^{-6}	5.35 × 10^{-6}	-4.00 × 10^{-6}
B_6^{-6}	-1.02 × 10^{-3}	-1.46 × 10^{-7}	-1.08 × 10^{-7}	2.65 × 10^{-2}	3.75 × 10^{-8}
B_6^{-5}	1.06 × 10^{-9}	5.18 × 10^{-10}	-7.29 × 10^{-10}	-3.23 × 10^{-10}	-3.65 × 10^{-8}
B_6^{-4}	-1.44 × 10^{-8}	5.12 × 10^{-3}	-1.06 × 10^{-8}	1.15 × 10^{-8}	-1.24 × 10^{-8}
B_6^{-3}	-7.24 × 10^{-10}	1.79 × 10^{-11}	1.24 × 10^{-10}	-3.79 × 10^{-10}	-1.63 × 10^{-10}
B_6^{-2}	1.12 × 10^{-9}	-1.43 × 10^{-8}	5.25 × 10^{-9}	-6.32 × 10^{-9}	4.73 × 10^{-9}
B_6^{-1}	2.07 × 10^{-10}	-2.96 × 10^{-11}	2.74 × 10^{-11}	-1.14 × 10^{-10}	-2.24 × 10^{-9}
B_6^0	**-2.23 × 10^{-3}**	**-3.60 × 10^{-3}**	**-3.58 × 10^{-3}**	**-3.68 × 10^{-3}**	**6.88 × 10^{-3}**
B_6^1	-8.28 × 10^{-11}	-6.85 × 10^{-11}	9.83 × 10^{-12}	-9.51 × 10^{-11}	2.39 × 10^{-9}
B_6^2	-5.26 × 10^{-8}	7.20 × 10^{-8}	-1.14 × 10^{-7}	-2.21 × 10^{-7}	-2.01 × 10^{-8}
B_6^3	1.23 × 10^{-10}	-1.62 × 10^{-10}	2.79 × 10^{-11}	6.68 × 10^{-10}	-3.92 × 10^{-9}
B_6^4	1.88 × 10^{-7}	**-4.23 × 10^{-2}**	1.20 × 10^{-7}	1.34 × 10^{-7}	2.07 × 10^{-7}
B_6^5	2.57 × 10^{-10}	-5.29 × 10^{-10}	3.82 × 10^{-11}	-2.03 × 10^{-9}	-2.60 × 10^{-8}
B_6^6	**3.44 × 10^{-2}**	6.70 × 10^{-7}	7.08 × 10^{-7}	**2.52 × 10^{-1}**	-4.73 × 10^{-7}

Table S49. Crystal field parameters from CASSCF calculations on the ErF_x series with bold parameters indicating truncated point group terms.

CFP	*ErF_3*	*ErF_4*	*ErF_5*	*ErF_6*
B_2^{-2}	-1.87 × 10^{-7}	-3.20 × 10^{-7}	2.38 × 10^{-6}	-3.24 × 10^{-6}
B_2^{-1}	-8.50 × 10^{-9}	-1.43 × 10^{-9}	-1.14 × 10^{-9}	2.70 × 10^{-8}
B_2^0	**-3.92**	**-5.43**	**-6.29**	**-7.58**
B_2^1	-1.00 × 10^{-8}	8.77 × 10^{-9}	1.29 × 10^{-8}	2.21 × 10^{-8}
B_2^2	-8.27 × 10^{-9}	-3.40 × 10^{-6}	-3.11 × 10^{-6}	3.00 × 10^{-6}
B_4^{-4}	-5.17 × 10^{-8}	-4.41 × 10^{-2}	9.27 × 10^{-8}	-1.83 × 10^{-8}
B_4^{-3}	-8.50 × 10^{-11}	6.47 × 10^{-11}	1.61 × 10^{-11}	1.85 × 10^{-10}
B_4^{-2}	3.26 × 10^{-9}	-3.02 × 10^{-8}	-2.40 × 10^{-8}	-2.78 × 10^{-8}
B_4^{-1}	-4.35 × 10^{-11}	1.10 × 10^{-10}	-7.29 × 10^{-11}	-2.24 × 10^{-10}
B_4^0	**3.21 × 10^{-3}**	**4.64 × 10^{-3}**	**4.45 × 10^{-3}**	**5.77 × 10^{-3}**
B_4^1	-1.07 × 10^{-10}	-4.84 × 10^{-12}	-1.00 × 10^{-10}	-1.87 × 10^{-10}
B_4^2	5.11 × 10^{-8}	2.15 × 10^{-8}	2.65 × 10^{-8}	-6.10 × 10^{-8}
B_4^3	1.30 × 10^{-10}	7.27 × 10^{-11}	7.53 × 10^{-12}	3.42 × 10^{-10}
B_4^4	-1.97 × 10^{-7}	**6.11 × 10^{-2}**	-2.26 × 10^{-8}	-6.72 × 10^{-9}
B_6^{-6}	1.72 × 10^{-4}	4.40 × 10^{-9}	-3.53 × 10^{-9}	8.47 × 10^{-4}
B_6^{-5}	-7.42 × 10^{-12}	-2.83 × 10^{-12}	1.38 × 10^{-11}	-1.24 × 10^{-11}
B_6^{-4}	-5.72 × 10^{-11}	4.33 × 10^{-4}	1.01 × 10^{-9}	4.15 × 10^{-9}
B_6^{-3}	1.05 × 10^{-12}	7.99 × 10^{-14}	-2.29 × 10^{-12}	3.70 × 10^{-13}
B_6^{-2}	2.04 × 10^{-10}	-5.37 × 10^{-10}	-5.19 × 10^{-10}	7.63 × 10^{-11}
B_6^{-1}	6.07 × 10^{-13}	-9.69 × 10^{-13}	1.43 × 10^{-12}	1.28 × 10^{-12}
B_6^0	**-3.47 × 10^{-5}**	**-5.89 × 10^{-5}**	**-6.34 × 10^{-5}**	**-7.08 × 10^{-5}**
B_6^1	3.01 × 10^{-12}	-7.94 × 10^{-13}	9.89 × 10^{-14}	1.53 × 10^{-12}
B_6^2	9.54 × 10^{-10}	1.73 × 10^{-9}	5.40 × 10^{-10}	3.25 × 10^{-10}
B_6^3	2.57 × 10^{-12}	-2.38 × 10^{-12}	-3.10 × 10^{-13}	-3.71 × 10^{-12}
B_6^4	-4.36 × 10^{-10}	**-6.00 × 10^{-4}**	-3.09 × 10^{-10}	1.49 × 10^{-9}
B_6^5	2.90 × 10^{-12}	2.11 × 10^{-13}	-7.15 × 10^{-12}	1.59 × 10^{-11}
B_6^6	**4.03 × 10^{-4}**	-3.04 × 10^{-10}	-1.61 × 10^{-9}	**3.20 × 10^{-3}**

Table S50. The anisotropy and τ_{QTM} attained from the calculations conducted by PHI for Yb(III) in ideal symmetries.

PHI Analysis	***g*-tensor *values***			**QTM from PHI**	**QTM from CASSCF**
	g_x	g_y	g_z	(s)	(s)
YbF_3	0.197	0.197	7.99	7.34×10^{-7}	1.3×10^{-6}
YbF_4	0.0311	0.0311	7.94	2.92×10^{-5}	3.33×10^{-5}
YbF_5	0	0	8.0	∞	3490
YbF_6	0.730	0.730	7.80	5.27×10^{-8}	4.14×10^{-8}
YbF_8	0	0	8.0	∞	198.81

Table S51. The anisotropy and τ_{QTM} attained from the calculations conducted by PHI for Er(III) in ideal symmetries.

PHI Analysis	***g*-tensor *values***			**QTM from PHI**	**QTM from CASSCF**
	g_x	g_y	g_z	(s)	(s)
ErF_3	9.09×10^{-17}	9.47×10^{-17}	17.996	7.47×10^{24}	9.61×10^{7}
ErF_4	4.26×10^{-3}	4.26×10^{-3}	17.94	3.53×10^{-3}	7.96×10^{-4}
ErF_5	0	0	18.0	∞	3.45×10^{10}
ErF_6	4.92×10^{-17}	7.16×10^{-17}	17.89	1.70×10^{25}	1.38×10^{5}

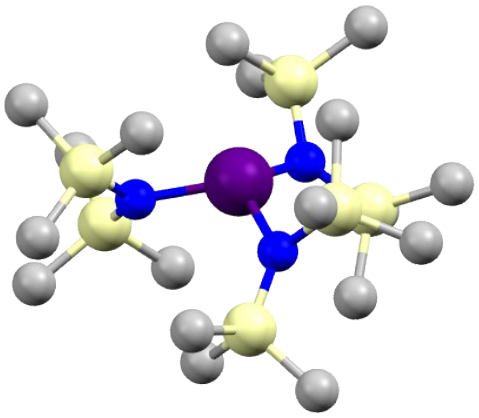

5. Comparison of a Real Trigonal Er(III) SMM and its Yb(III) Analogue

Figure S7. Distorted D_{3h} structure of [Ln{N(Me$_3$Si)$_2$}$_3$]

Table S52. The anisotropy, GS wavefunction decomposition, U_{eff}, and $^{\tau_{QTM}}$ for [Er{N(Me$_3$Si)$_2$}$_3$]

Crystal field		***g*-tensor values**			**Angle**	**Wavefunction decomposition**
Energy (cm^{-1})	**Energy (K)**	**g_x**	**g_y**	**g_z**	(°)	
0	0	2.05 x 10^{-5}	2.17 x 10^{-5}	17.88	--	99.6%|∓15/2⟩; 0.4%|∓9/2⟩;
110	157	0.140	0.140	15.46	0	99.7%|±13/2⟩; 0.2%|±7/2⟩; 0.1%|±1/2⟩;
197	281	0.138	0.139	12.79	0	96.1%|±11/2⟩; 3.3%|±5/2⟩; 0.6%|∓1/2⟩;
273	390	0.024	0.025	9.905	0	89.7%|±9/2⟩; 10.0%|±3/2⟩; 0.4%|±15/2⟩;
339	484	5.91	5.90	5.86	27	76.8%|∓7/2⟩; 12.4%|∓1/2⟩; 10.3%|±5/2⟩; 0.3%|±11/2⟩; 0.1%|∓13/2⟩;
450	643	5.88	5.81	3.69	90	74.2%|±5/2⟩; 11.9%|∓7/2⟩; 10.7%|∓1/2⟩; 3.1%|±11/2⟩; 0.1%|∓13/2⟩;
515	736	0.114	0.205	3.98	2	90.0%|±3/2⟩; 9.9%|±9/2⟩;
556	794	9.54	9.18	1.06	90	76.2%|∓1/2⟩; 12.1%|±5/2⟩; 11.1%|∓7/2⟩;

						0.5%|±11/2⟩; 0.1%|∓13/2⟩;

Table S53. The anisotropy, GS wavefunction decomposition, U_{eff}, and τ_{QTM} for $[Yb\{N(Me_3Si)_2\}_3]$

Crystal field		***g*-tensor values**			**Angle**	**Wavefunction decomposition**
Energy (cm^{-1})	**Energy (K)**	**g_x**	**g_y**	**g_z**	(°)	
0	0	0.175	0.175	7.94	--	99.6%|±7/2⟩; 0.3%|±1/2⟩; 0.1%|∓5/2⟩;
777	1110	0.167	0.168	5.63	0	99.7%|±5/2⟩; 0.3%|∓1/2⟩; 0.1%|∓7/2⟩;
1221	1745	0.0323	0.0332	3.3882	0	100.0%|∓3/2⟩;
1444	2063	4.58	4.51	1.131	90	99.4%|±1/2⟩; 0.3%|∓5/2⟩; 0.3%|±7/2⟩;

6. Predictions of Experimental Targets

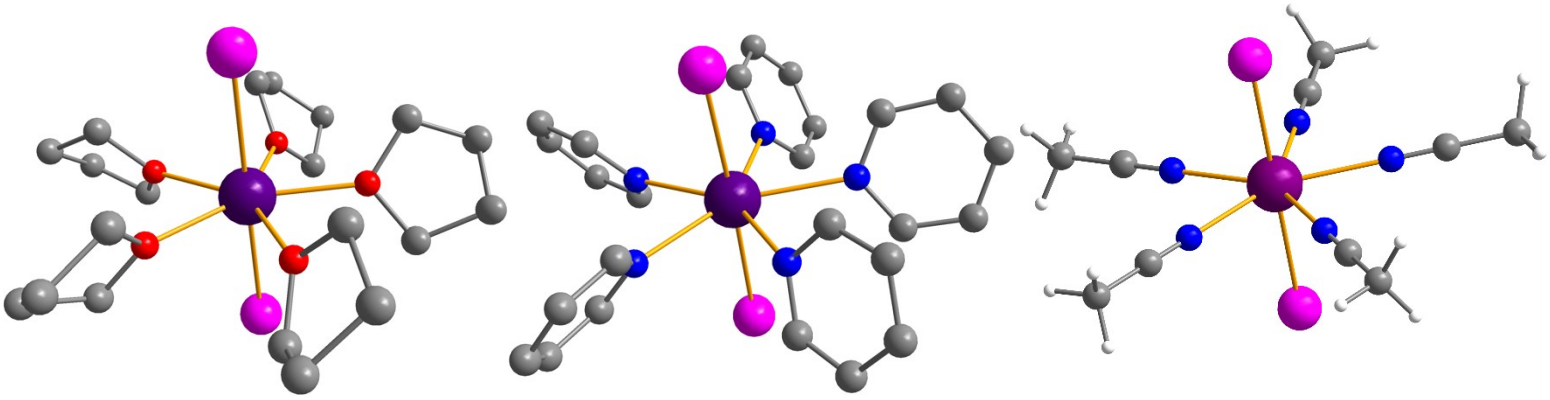

Figure S8. Known 7-coordinated Yb(III) environments with the chemical formulae of $[YbI_2(X)_5]^+$.

Table S54. The anisotropy, GS wavefunction decomposition, U_{eff}, and τ_{QTM} for $[YbI_2(X)_5]^+$ complexes.

	g*-tensor *values			**Wavefunction Decomposition**	***U*eff**	**QTM**
	g_x	***g_y***	***g_z***		(K)	(s)
1-$[YbI_2(THF)_5]^+$	5.20×10^{-3}	7.80×10^{-3}	7.97	99.9%$\|\pm 7/2\rangle$; 0.1% $\|\mp 3/2\rangle$	693	6.48×10^{-4}

2-[$YbI_2(THF)_5$]$^+$	1.51×10^{-2}	1.81×10^{-2}	7.97	99.9%$\lvert \pm 7/2\rangle$; 0.1% $\lvert \mp 3/2\rangle$	714	1.02×10^{-4}
[$YbI_2(Py)_5$]$^+$	3.30×10^{-2}	3.72×10^{-2}	7.98	99.9%$\lvert \pm 7/2\rangle$	675	2.30×10^{-5}
[$YbI_2(MeCN)_5$]$^+$	1.56×10^{-5}	1.56×10^{-5}	7.98	100%$\lvert \pm 7/2\rangle$	95	118

Table S55. Crystal field properties resulted from CASSCF-SO calculations for a 7-coordinated known structure of **1-[$YbI_2(THF)_5$]$^+$**.

Crystal field		***g*-tensor values**			**Angle**	**Wavefunction decomposition**
Energy (cm^{-1})	**Energy (K)**	**g_x**	**g_y**	**g_z**	(°)	
0	0	5.20×10^{-3}	7.80×10^{-3}	7.97	--	99.9%$\lvert \pm 7/2\rangle$; 0.1% $\lvert \mp 3/2\rangle$
438	631	0.251	0.253	5.60	10	95.8%$\lvert \pm 5/2\rangle$; 3.1%$\lvert \pm 1/2\rangle$; 1%$\lvert \pm 3/2\rangle$
482	693	1.75	3.23	4.82	83	63.1%$\lvert \pm 3/2\rangle$; 31.8% $\lvert \mp 1/2\rangle$; 2.1%$\lvert \pm 1/2\rangle$; 1.4%$\lvert \pm 5/2\rangle$; 1.1% $\lvert \mp 5/2\rangle$; 0.3% $\lvert \mp 3/2\rangle$
505	727	0.515	0.937	7.55	90	50%$\lvert \mp 1/2\rangle$; 33.1%$\lvert \pm 3/2\rangle$; 12.9%$\lvert \pm 1/2\rangle$; 2.3% $\lvert \mp 3/2\rangle$; 1.6% $\lvert \mp 5/2\rangle$

Table S56. Crystal field properties resulted from CASSCF-SO calculations for the second 7-coordinated known structure of **2-[$YbI_2(THF)_5$]$^+$**.

Crystal field		***g*-tensor values**			**Angle**	**Wavefunction decomposition**
Energy (cm^{-1})	**Energy (K)**	**g_x**	**g_y**	**g_z**	(°)	
0	0	1.51×10^{-2}	1.81×10^{-2}	7.97	--	99.9%$\lvert \pm 7/2\rangle$; 0.1% $\lvert \mp 3/2\rangle$
446	642	0.202	0.342	5.72	12	96.6%$\lvert \pm 5/2\rangle$; 2.7%$\lvert \pm 3/2\rangle$; 0.6%$\lvert \pm 1/2\rangle$; 0.1% $\lvert \mp 3/2\rangle$
496	714	1.98	3.65	3.77	66	63.7%$\lvert \pm 3/2\rangle$; 24.5% $\lvert \pm 1/2\rangle$; 10.1%$\lvert \mp 1/2\rangle$; 1.0%$\lvert \pm 5/2\rangle$; 0.4% $\lvert \mp 5/2\rangle$; 0.3% $\lvert \mp 3/2\rangle$
521	750	0.344	0.584	7.17	77	54.4%$\lvert \pm 1/2\rangle$; 31.2%$\lvert \pm 3/2\rangle$; 10.3% $\lvert \mp 1/2\rangle$; 2.0% $\lvert \mp 3/2\rangle$; 2.0%$\lvert \pm 5/2\rangle$

Table S57. Crystal field properties resulted from CASSCF-SO calculations for a 7-coordinated known structure of **$[YbI_2(Py)_5]^+$**.

Crystal field		***g*-tensor values**			**Angle**	**Wavefunction decomposition**
Energy (cm^{-1})	**Energy (K)**	**g_x**	**g_y**	**g_z**	(°)	
0	0	3.30×10^{-2}	3.72×10^{-2}	7.98	--	99.9%$\vert \pm 7/2\rangle$;
426	613	0.575	0.784	5.58	12	95.1%$\vert \pm 5/2\rangle$; 3.1%$\vert \pm 1/2\rangle$; 1.3%$\vert \pm 3/2\rangle$; 0.5%$\vert \mp 3/2\rangle$
484	697	2.41	2.91	3.43	86	80.2.%$\vert \pm 3/2\rangle$; 14.8% $\vert \mp 1/2\rangle$; 1.7%$\vert \pm 5/2\rangle$; 1.7% $\vert \mp 5/2\rangle$; 1.4%$\vert \pm 1/2\rangle$; 0.2% $\vert \mp 3/2\rangle$
526	756	0.528	1.06	7.33	89	74.9%$\vert \pm 1/2\rangle$; 12.8% $\vert \mp 3/2\rangle$; 5.7% $\vert \mp 1/2\rangle$; 4.9%$\vert \pm 3/2\rangle$; 1.3%$\vert \pm 5/2\rangle$; 0.4%$\vert \mp 5/2\rangle$

Table S58. Crystal field properties resulted from CASSCF-SO calculations for an idealised 7-coordinated known structure of **$[YbI_2(MeCN)_5]^+$** with a fixed Yb-N bond distance 2.395 Å.

Crystal field		***g*-tensor values**			**Angle**	**Wavefunction decomposition**
Energy (cm^{-1})	**Energy (K)**	**g_x**	**g_y**	**g_z**	(°)	
0	0	1.56×10^{-5}	1.56×10^{-5}	7.98	--	100%$\vert \pm 7/2\rangle$
66	95	4.56	4.56	1.14	0	100%$\vert \pm 1/2\rangle$
104	150	3.02×10^{-4}	3.73×10^{-4}	3.44	0	100%$\vert \pm 3/2\rangle$
180	259	1.89×10^{-5}	5.24×10^{-5}	5.70	0	100%$\vert \pm 5/2\rangle$

Table S59. Crystal field properties resulted from CASSCF-SO calculations for an idealised 7-coordinated known structure of $[YbI_2(MeCN)_5]^+_{short}$ with Yb-N bond distance 2.221 Å.

Crystal field		***g*-tensor values**			**Angle**	**Wavefunction decomposition**
Energy (cm^{-1})	**Energy (K)**	**g_x**	**g_y**	**g_z**	(°)	
0	0	1.34×10^{-5}	1.34×10^{-5}	7.96	--	100%$\vert \pm 7/2\rangle$
386	556	1.86×10^{-5}	3.92×10^{-4}	3.44	0	100%$\vert \pm 3/2\rangle$
413	594	1.73×10^{-4}	2.00×10^{-4}	5.68	0	100%$\vert \pm 5/2\rangle$
421	606	4.55	4.55	1.13	0	100%$\vert \pm 1/2\rangle$

Table S60. Crystal field properties resulted from CASSCF-SO calculations for an empirically optimised 7-coordinated structure of $[YbI_2(MeCN)_5]^+_{opt}$.

Crystal field		***g*-tensor values**			**Angle**	**Wavefunction decomposition**
Energy (cm^{-1})	**Energy (K)**	**g_x**	**g_y**	**g_z**	(°)	
0	0	0.151	0.389	7.60	--	96.2%$\vert \pm 7/2\rangle$; 2.96%$\vert \mp 3/2\rangle$
314	452	1.51	3.28	5.40	0	41.0%$\vert \pm 5/2\rangle$; 35.4%$\vert \mp 3/2\rangle$; 23.2%$\vert \pm 1/2\rangle$
333	479	1.90	2.07	3.16	0	47.6%$\vert \pm 1/2\rangle$; 46.3%$\vert \pm 5/2\rangle$; 6.03%$\vert \mp 3/2\rangle$
385	554	1.49	2.39	5.77	0	55.6%$\vert \pm 3/2\rangle$; 28.7%$\vert \mp 1/2\rangle$; 12.4%$\vert \mp 5/2\rangle$

References:

1 J. J. Zakrzewski, K. Kumar, M. Zychowicz, R. Jankowski, M. Wyczesany, B. Sieklucka, S. I. Ohkoshi and S. Chorazy, *Journal of Physical Chemistry Letters*, 2021, **12**, 10558–10566.

2 H. Allia, A. Rodríguez-Expósito, M. A. Palacios, J. R. Jiménez, A. N. Carneiro Neto, R. T. Moura, F. Piccinelli, A. Navarro, M. M. Quesada-Moreno and E. Colacio, *Physical Chemistry Chemical Physics*, 2025, **27**, 13266–13279.

3 M. Wang, X. Wei, J. Zhu, J. Wang, M. Wang, L. Liu, T. Sun and Y. Tang, *J. Solid State Chem.*, 2020, **283**, 121172.

4 W. Huang, J. Xu, D. Wu, X. Huang and J. Jiang, *New Journal of Chemistry*, 2015, **39**, 8650–8657.

5 S. Chorazy, M. Zychowicz, S. I. Ohkoshi and B. Sieklucka, *Inorg. Chem.*, 2019, **58**, 165–179.

6 D. Q. Wu, D. Shao, X. Q. Wei, F. X. Shen, L. Shi, Y. Q. Zhang and X. Y. Wang, *Dalton Transactions*, 2017, **46**, 12884–12892.

7 Y. Li, J. W. Yu, Z. Y. Liu, E. C. Yang and X. J. Zhao, *Inorg. Chem.*, 2015, **54**, 153–160.

8 J. R. Jiménez, I. F. Díaz-Ortega, E. Ruiz, D. Aravena, S. J. A. Pope, E. Colacio and J. M. Herrera, *Chemistry - A European Journal*, 2016, **22**, 14548–14559.

9 A. Gorczyński, D. Marcinkowski, M. Kubicki, M. Löffler, M. Korabik, M. Karbowiak, P. Wiśniewski, C. Rudowicz and V. Patroniak, *Inorg. Chem. Front.*, 2018, **5**, 605–618.

10 D. Zeng, M. Ren, S. S. Bao, Z. S. Cai, C. Xu and L. M. Zheng, *Inorg. Chem.*, 2016, **55**, 5297–5304.

11 B. Lefeuvre, J. Flores Gonzalez, F. Gendron, V. Dorcet, F. Riobé, V. Cherkasov, O. Maury, B. Le Guennic, O. Cador, V. Kuropatov and F. Pointillart, *Molecules*, 2020, **25**, 492.

12 Y. Xin, K. Kumar, J. J. Zakrzewski, S. Chorazy, K. Nakabayashi, O. Stefanczyk and S. I. Ohkoshi, *Journal of Physical Chemistry C*, 2023, **127**, 15500–15511.

13 A. Borah, S. Dey, S. K. Gupta, M. G. Walawalkar, G. Rajaraman and R. Murugavel, *Chemical Communications*, 2020, **56**, 11879–11882.

14 S. D. Zhu, J. J. Hu, L. Dong, H. R. Wen, S. J. Liu, Y. B. Lu and C. M. Liu, *J. Mater. Chem. C Mater.*, 2020, **8**, 16032–16041.

15 T. P. Latendresse, V. Vieru, A. Upadhyay, N. S. Bhuvanesh, L. F. Chibotaru and M. Nippe, *Chem. Sci.*, 2020, **11**, 3936–3951.

16 M. Ren, Z. L. Xu, S. S. Bao, T. T. Wang, Z. H. Zheng, R. A. S. Ferreira, L. M. Zheng and L. D. Carlos, *Dalton Transactions*, 2016, **45**, 2974–2982.

17 B. Casanovas, M. Font-Bardía, S. Speed, M. S. El Fallah and R. Vicente, *Eur. J. Inorg. Chem.*, 2018, **2018**, 1928–1937.

18 J. L. Liu, K. Yuan, J. D. Leng, L. Ungur, W. Wernsdorfer, F. S. Guo, L. F. Chibotaru and M. L. Tong, *Inorg. Chem.*, 2012, **51**, 8538–8544.

19 K. Soussi, J. Jung, F. Pointillart, B. Le Guennic, B. Lefeuvre, S. Golhen, O. Cador, Y. Guyot, O. Maury and L. Ouahab, *Inorg. Chem. Front.*, 2015, **2**, 1105–1117.

20 L. Maxwell, M. Amoza and E. Ruiz, *Inorg. Chem.*, 2018, **57**, 13225–13234.

21 F. Guégan, J. Jung, B. Le Guennic, F. Riobé, O. Maury, B. Gillon, J. F. Jacquot, Y. Guyot, C. Morell and D. Luneau, *Inorg. Chem. Front.*, 2019, **6**, 3152–3157.

22 M. Sugita, N. Ishikawa, T. Ishikawa, S. Y. Koshihara and Y. Kaizu, *Inorg. Chem.*, 2006, **45**, 1299–1304.

23 C. A. Mattei, V. Montigaud, B. Lefeuvre, V. Dorcet, G. Argouarch, O. Cador, B. Le Guennic, O. Maury, C. Lalli, Y. Guyot, S. Guy, C. Gindre, A. Bensalah-Ledoux, F. Riobé, B. Baguenard and F. Pointillart, *J. Mater. Chem. C Mater.*, 2023, **11**, 7299–7310.
24 N. Jain, F. Houard, R. Marchal, M. Cordier, B. Le Guennic, Y. Suffren, Y. Sarazin and K. Bernot, *ChemistryEurope*, 2024, **2**, e202400062.
25 D. Errulat, K. L. M. Harriman, D. A. Gálico, A. A. Kitos, A. Mansikkamäki and M. Murugesu, *Nat. Chem.*, 2023, **15**, 1100–1107.
26 M. Liberka, K. Boidachenko, J. J. Zakrzewski, M. Zychowicz, J. Wang, S. Ohkoshi and S. Chorazy, *Magnetochemistry*, 2021, **7**, 79.
27 J. González, V. K. Fagundes, M. A. Hay, E. Dallerba, M. Massi, C. R. Hall, M. J. Giansiracusa and C. Boskovic, *Dalton Transactions*, 2026, **55**, 1792
28 P. Richardson, R. Marin, Y. Zhang, B. Gabidullin, J. Ovens, J. O. Moilanen and M. Murugesu, *Chemistry - A European Journal*, 2021, **27**, 2361–2370.
29 K. Karachousos-Spiliotakopoulos, V. Tangoulis, N. Panagiotou, A. Tasiopoulos, E. Moreno-Pineda, W. Wernsdorfer, M. Schulze, A. M. P. Botas and L. D. Carlos, *Dalton Transactions*, 2022, **51**, 8208–8216.
30 S. Bagio, J. González, R. W. Gable, C. R. Hall, C. Boskovic and M. J. Giansiracusa, *Dalton Transactions*, 2025, **54**, 5061–5074.
31 K. Kumar, O. Stefanczyk, K. Nakabayashi, K. Imoto, Y. Oki and S. Ohkoshi, *Adv. Opt. Mater.*, 2022, **10**, 202101721